ASTRONOMY & ASTROPHYSICS
SUPPLEMENT SERIES

JUNE I **1999**, PAGE 273

Astron. Astrophys. Suppl. Ser. **137**, 273–292 (1999)

Search for reference A0 dwarf stars: Masses and luminosities revisited with Hipparcos parallaxes⋆,⋆⋆

M. Gerbaldi[1,2], R. Faraggiana[3], R. Burnage[4], F. Delmas[1], A.E. Gómez[5], and S. Grenier[5]

[1] CNRS, Institut d'Astrophysique, 98bis, Bd. Arago, 75014 Paris, France
[2] Université de Paris-Sud XI, Paris, France
[3] Dipartimento di Astronomia, Università degli Studi di Trieste, v. Tiepolo 11, 34131 Trieste, Italy
[4] CNRS, Observatoire de Haute-Provence, 04870 Saint Michel l'Observatoire, France
[5] DASGAL, Observatoire de Paris-Meudon, Place Janssen, 92195 Meudon Cedex, France

Received November 12, 1998; accepted March 1, 1999

Abstract. Hipparcos data for 71 nearby dwarf A0 stars were combined with other data, in particular with high resolution spectra to establish the HR diagram in this temperature range. Almost 30% of unknown binaries were detected and discarded before establishing the $\mathcal{M}$-L relation for bright A0 V field stars. The relationship derived for these single stars is compared to the classical diagram derived from eclipsing binaries. The scatter of the latter is examined and the role of gravity is discussed.

A good agreement is found between the evolution-based surface gravity $\log g_{\rm ev}$ and the value of $\log g_{\rm ph}$ obtained from photometric data.

Key words: stars: fundamental parameters — stars: early type — stars: HR diagram

1. Introduction

The access to precise Hipparcos parallaxes opens the possibility to go further in the knowledge of astrophysical stellar parameters when these parallaxes are coupled with other data.

The luminosity function of early-type stars allows to study the recent history of our Galaxy up to about 1 Gyr. We have selected the A0-type stars as representative of young objects which are long-lived enough on the main sequence to be present, in significant percentage, in the solar neighbourhood.

On one hand the use of field stars has the advantage, compared to cluster stars, to provide a larger sample of bright stars for which more accurate photometric and spectroscopic data can be obtained. On the other hand the use of field stars requires the knowledge of precise individual distances.

The present study is based on a sample of 71 A0 stars. This sample is extracted from a large set of data collected in the framework of an ESO Key Program (Gerbaldi et al. 1989), for studying B8 to F2 stars belonging to the Hipparcos Input Catalogue (Turon et al. 1992). These stars are classified non supergiant A0 in the Bright Star Catalogue (Hoffleit & Jaschek 1982) [hereafter named BSC]; for the few stars not belonging to the BSC, the spectral type is taken from the CDS data base. Stars classified as Ap and Am stars were discarded from the observational program. Among these 71 stars (limited to the Southern Hemisphere) 50 are classified A0 V and represent 21% of the BSC A0 V stars; these stars are expected to be at a distance $d \leq 150$ pc.

The purpose of this study is to select a reference sample of non supergiant A0 stars to be used for the construction of an accurate HR diagram where M_V is derived from the Hipparcos parallaxes.

The spectroscopic observations are used to verify, through the comparison between observed and computed spectra, the accuracy of the photometrically derived atmospheric parameters; several criteria are used to detect possible peculiarities.

The determination of $T_{\rm eff}$ and $\log g$ is discussed in Sect. 3; the computations of the grid of synthetic spectra and the fit on the observed ones are described in Sect. 4; the results obtained from the spectral analysis are

Send offprint requests to: M. Gerbaldi

⋆ Based on observations collected at the European Southern Observatory (ESO), La Silla, Chile in the framework of the Key Programme 5-004-43K and on data from the ESA Hipparcos astrometry satellite.

⋆⋆ The Tables 1-4 are also available electronically via anonymous ftp 130.79.128.5 or via http://cdsweb.u-strasbg.fr/Abstract.html

presented in Sects. 5 and 6. A subsample of non binary, non peculiar stars is defined (Sect. 7) for which the resulting HR diagram is discussed in Sect. 8.1; in Sect. 8.2 the gravity derived from atmospheric properties (photometric and spectroscopic data) are compared with that obtained combining stellar evolution models and luminosity computed from the Hipparcos parallaxes. In Sect. 8.3 the Mass-Luminosity relationship is analyzed and compared to the empirical one, derived from the eclipsing binaries.

2. Observations and data reduction

The basic data on the observed stars have been gathered in Table 1. Star identifications are given in Cols. 1 and 2, the spectral types from the BSC and from Abt and Morrell (1995) (hereafter AM) in Cols. 3 and 4.

The list of the established double stars in this sample can be extracted from the informations given in Annex 1 of the Hipparcos Input Catalogue (Turon et al. 1992), as well as from the Hipparcos and Tycho Catalogues (ESA, 1997) for the new ones discovered during this mission. For visual doubles the magnitude difference and the angular separation, given in Cols. 5 and 6, are for the systems for which these values can affect the measures. These informations are given in the last column of Table 1. Results from search for binarity by speckle observations (Col. 7) are taken from the update of the Bright Star Catalogue (Hoffleit & Warren 1994) [hereafter named BSC1994], kindly communicated by W.H. Warren. Projected rotational velocities, according to the BSC and to AM are added in Cols. 8 and 9.

The spectra were obtained with the ECHELEC spectrograph mounted at the ESO 1.5 m telescope, in the period Jan. 89 - Jan. 95. The linear dispersion is about 3.1 Å mm^{-1} in the chosen wavelength range 4210−4500 Å. The slit width of 320 μm corresponds to 1.52 arcsec on the sky. From unblended thorium lines, the FWHM of the instrumental profile was measured; its value is 0.17 Å, in agreement with the size of the entrance slit. The original frame covers 11 orders of the echelle spectrum; only 9 of them have been retained and reduced, while the 2 truncated orders on both sides of the central wavelength have been discarded. Flat field correction with a tungsten lamp and wavelength calibration with a Th lamp have been made with classical procedures. Great care was devoted to remove instrumental defects which arose from time to time: the most important ones were the two ghosts present as transversal bars on the original frames in the 1991-1994 period; the method is based on the accurate analysis of the intensity in the inter-orders. The resolution is about 28 000 and the S/N, highly variable from the center to the edges of each order, covers the range 50 to 200.

The analysis of the H_γ profile being one of the goals of the present study, we had to produce a single spectrum by interconnecting the echelle orders. A particular attention was given to the method adopted for this connection. The complete reduction procedure is described in Burnage & Gerbaldi (1990, 1992). The broad spectral domain covered by the H_γ line in A0 dwarf stars imposes to give a particular attention to the procedure adopted to normalize the spectra. The normalization is made by trial and error method; first the spectra have been normalized in the classical way by drawing the continuum through the highest points of the spectrum and then overplotted on a template synthetic spectrum. This allows to choose a number of continuum points common to both; these points are used as references in the final normalization procedure.

Since the observations span over 5 years, we have systematically observed four stars. The number of spectra obtained for each of them are: HD 15371: 19 spectra, HD 48915 (Sirius): 31 spectra, HD 149348: 13 spectra, HD 193924: 15 spectra. We checked the instrumental stability of the spectrograph and the consistency of the reduction procedures through the comparison of the spectra of these stars.

The reliability of the photometric calibration given by the flat field correction has been investigated through the measurement of the equivalent width (hereafter written EW) of lines selected over the observed spectral range; the number of lines measured in each spectrum was: 9 for HD 15371, 29 for HD 48915, 15 for HD 149348 and 6 for HD 193924. For each of these stars, we controlled that the distribution of the EWs of the selected lines is Gaussian; the mean value of the EW for each of these lines has been computed and the mean value of all the standard deviation is smaller than 0.005 Å.

The mechanical stability of the instrument has been tested through the measurement of the position of the same set of lines in the same stars. The final result is that the rms of line wavelengths corresponds to 1 $km\,s^{-1}$.

We verified also, using all the spectra of HD 48915, that the profile shape, after the normalization of the spectra, is conserved whatever the setup of the spectrograph has been.

These necessary tests allow us to use confidently the whole set of observations as an homogeneous sample of data in the following analysis.

3. Determination of $T_{\rm eff}$, $\log g$

For large samples of stars, the best method for $T_{\rm eff}$, $\log g$ determination is based on the use of calibrated photometric indices. For early-type stars the $uvby\beta$ and Geneva photometric systems are the most commonly used. In the $uvby\beta$ photometric system specific filters measure the strength of the Hβ line.

We have determined $T_{\rm eff}$ and $\log g$ using calibrations of both photometric systems. A non systematic discrepancy

Table 1. The programme stars

HD	HR	Sp(BSC)	Sp(AM)	Δm	Sep arcsec	Speckle arcsec	Rot(BSC) km s^{-1}	Rot(AM) km s^{-1}	Remarks
3003	136	A0 V	A1 IV	0.2	0.1		84	...	
4065	185	A0 V	–	0.3	0.7	0.731	–	–	Hipparcos 0.43 mag 0.737 arcsec
4150	191	A0 IV	A0 IV				–	...	
7916	380	A0 V		2.4	2.4		–	–	Hipparcos 1.95 mag 2.435 arscsec
15004	704	A0 III	B9 III:n + shell (HI)				–	200	
15646	734	A0 V					–	–	
16152	–	A0					–	–	
17864	853	A0 V					–	–	Hip. *new binary* 3.82 mag 0.314 arcsec
18735	903	A0 V					–	–	
20980	1018	A0 V	A1 V				–	35	
21473	1049	A0 V					–	–	
22789	1114	A0 V	A0 V				–	135	
27660	–	A0					–	–	
30397	1524	A0 V					–	–	
31295	1570	A0 V	A0 Vp (λBoo)				104	105	
32996	1661	A0 V	A1 Vp (Si st,Ca wk)				$\leq$41	15	
34868	1758	A0 V	A1 IV				69	90	
34968	1762	A0 Vv	B9 III	3.8	4.2		51	70	Hipparcos 3.72 mag 4.108 arcsec
36473	1849	A0 V	A0 V				60	45	
38056	1966	A0 V					–	–	
38206	1975	A0 Vs	A0 IIIs			negative	$\leq$41	25	
42301	2180	A0 IV	A0 Vn				–	225:	
42729	2206	A0 V	B9.5 V				–	20	
42834	2211	A0 V					–	–	
45557	2345	A0 V	A0 V				–	...	
47827	2455	A0	B9.5 Vp (4481 wk)	0.4	0.1	0.058*	–	15	* = speckle from Hartkopf et al. (1996)
56341	2755	A0	A0 V				–	35	
60629	2912	A0 V	A0.5 III				–	40	
63112	3019	A0 V				negative	$\leq$41	–	
63584	3038	A0 IV-V					–	–	
67725	3189	A0 Vn	A0 Vp (4481 wk)			negative	160	...	
69589	3255	A0	A1 IV				–	110	
71043	3300	A0 V					–	–	
71155	3314	A0 V	A0 V			negative	125	115	
71576	3334	A0-1 IV-V					–	–	
74475	3463	A0 V					–	–	
76346	3549	A0 V					–	–	
79108	3651	A0 V	A0 Vp (λBoo)			negative	150	160	
80950	3721	A0 V					–	–	
84461	3875	A0 IV					16	–	
85504	3906	A0 Vs	B9.5 III			negative	$\leq$41	15	
87344	3963	A0 V	B9 IV			negative	17	15	
87363	3964	A0 V					–	–	
87887	3981	A0 III	B9.5 III				9	10	
92845	4194	A0 V					131	–	
97585	4356	A0 V	B9.5 Vn			negative	177	175	
99922	4428	A0 V		3.0	8.3		–	–	Hipparcos 3.31 mag 8.185 arcsec
101615	4502	A0 V					0	–	
104039	4579	A0-1 V	A1 IIIs	0.2	0.2		0	$<$10	
104430	4592	A0 V					–	–	
106797	4669	A0 V					–	–	
109573	4796	A0				negative	–	–	
111519	4871	A0 V*					–	–	* = A0 Vm (BSC, 1994)
111786	4881	A0 III	F0 Vp (λBoo,met:A1)				–	135	
113852	4947	A0 IV-III					$\leq$49	–	
114570	4977	A0 Vm:					–	–	
125473	5367	A0 IV	B9.5 V				101	...	
129791	–	A0 V					–	–	
139129	5798	A0 V					0	–	
151527	6235	A0 Vn	B9.5 Vp (4481wk)n			negative	139	225:	
152849	6291	A0 V	A0 Vn	0.3	1.1	0.993	–	190	Hipparcos 0.35 mag 0.998 arcsec
160263	6572	A0 V					–	–	
170680	6944	A0 Vn*	A0 Vp (λBoo)			negative	213	200:	* = A0 Vp (BSC, 1994)
188228	7590	A0 V	A0 IV				110	...	
193571	7779	A0 V				negative	–	–	
213320	8573	A0 IVs	A0 III				23	10	Hip. *new binary* 3.60 mag 3.744 arcsec
213398	8576	A0 V	A1 III			negative	36	...	
216931	–	A0					–	–	
218639	8816	A0 Vn	A0 Vn				154	235:	
223352	9016	A0 V	A0 Vp (λBoo)n				–	280:	
225200	9102	A0 V	B9 IVs + A2n				–	315:	

between the the two sets of values will be used as an additional information to interpret the spectra. We adopted the Moon & Dworetsky (1985) [hereafter MD] and Künzli et al. (1997) calibrations for $uvby\beta$ and Geneva systems respectively.

The homogenized $uvby\beta$ colours are taken from the Hauck & Mermilliod (1990) Catalogue [hereafter HM] and are given in Cols. 2 to 5 of Table 2. In this catalogue the Strömgren indices are erroneous for HD 225200 (Geneva code = 409010021) and we adopted the values from the Simbad data base. The indices are missing for the 2 stars HD 27660 and HD 216931 and we checked that there is no update in the recent edition by Mermilliod et al. (1997). The reddening of these stars has been estimated from the UBV indices: it is negligible for the first star and $E(B-V) = 0.06$ is derived for the second one. We also note that the secondary component of the broad visual double HD 87344, indicated as HD 87344(2) (V = 8.0), in the Hauck and Mermilliod Catalogue is in reality HD 87330 (V = 7.13, B9III-IV). Its spectrum clearly shows that the star HD 87330 is an SB2 with a well developed system of double lines at the epoch of our observations (May 13, 1990 and April 8, 1993).

For the Geneva photometry the version of the Catalogue available at CDS has been used. HD 129791 is not included in this Catalogue.

We recall that as a first step dereddened colours must be computed; for our sample of stars, dereddening is expected to be very low or negligible; a strong reddening is likely to indicate a flux distortion due to spectral peculiarities or undetected binarity.

3.1. Reddening and its correction

For these bright stars, mainly belonging to the BSC, standard methods of dereddening are assumed to be valid, these stars being expected to be slightly reddened. We used the programs by Moon (1985) to compute the colour excess. A similar determination cannot be performed from the Geneva photometric indices because no updated procedures are published.

The A-type stars are in the domain where the Balmer lines reach their maximum. According to Strömgren (1966), the $uvby\beta$ calibration requires that each star should be assigned to one of the three groups: early (β depends mainly on the luminosity, c_0 is mainly related to the $T_{\rm eff}$), late (the roles of β and c_0 are reversed) or intermediate (for which a combination of various indices must be used). In the program UVBYBETA by Moon (1985) the choice of the group is based on photometric quantities and spectral classification. Since the boundaries between the groups overlap in some cases, the assignment to a group is sometimes ambiguous and uncertainty in group selection cannot be avoided. In this case, the computations have been made for both groups; the result is an average difference of 0.02 in the colour excess $E(b-y)$. Details concerning this effect can be found in Gerbaldi et al. (1998a). The final choice of the group defined in the UVBYBETA program is given in Col. 6 of Table 2; this choice is made on the basis of the lower $E(b-y)$ and by the analysis of the atmospheric parameters derived for both cases (see next subsection).

The determination of the amount of reddening, being based on the empirical calibration of the $uvby\beta$ system, is model independent. However, the intrinsic colours are slightly different according to different authors and this may lead to different values of the colour excess; a discussion on this effect can be found in Figueras et al. (1991) and in Jordi et al. (1997). According to these papers, for our sample of nearby stars, we can safely use the Moon program UVBYBETA without any further modification.

The value of $E(b-y)$ is given in Col. 7 of Table 2. Only 6 stars have $E(b-y)$ higher than 0.02; to this we can add the estimated value for HD 216931. The highest value, $E(b-y) = 0.05$, is found only in one case, for HD 151527, which with HD 111786 [$E(b-y) = 0.00$] are the only two stars to present the peculiarity of a $(b-y)$ index very high for stars belonging to the A0 type. These two newly detected binaries are further discussed below. For the three stars HD 7916, HD 114570 and HD 129791 the colour excess is $E(b-y) = 0.04$; for two others HD 67725, HD 104039 the value of the colour excess is $E(b-y) = 0.03$.

For the remaining stars the $E(b-y)$ is what expected, i.e. in the range -0.01, $+0.02$, with the exception of HD 60629, which has a slightly higher "blueing" $E(b-y) = -0.02$. These values of reddening and bluing are interpreted as possible sign of abnormality. These stars will be discussed in Sect. 7.

3.2. $T_{\rm eff}$ and $\log g$ from $uvby\beta$ photometry

The atmospheric parameters have been derived from the $uvby\beta$ photometry, using the calibration by Moon & Dworetsky (1985) (Table 2, Cols. 8 and 9) which has been tested by recent studies (Napiwotzki et al. 1993; Smalley & Dworetsky 1993, for stars cooler than A0). The corrections determined by Castelli (1991) and by Dworetsky & Moon (1986) have no influence on our range of parameters.

The internal errors on $T_{\rm eff}$ and $\log g$ due to the scatter of the individual observed colours have been estimated by Lemke (1989) to be approximately $\pm$100 K and $\pm$0.1 dex respectively. A different approach to the evaluation of these errors is found in Gerbaldi et al. (1998b), where it is shown that a difference of 0.015 in colour excess implies a difference of 200 K in $T_{\rm eff}$.

Table 2. Photometric, astrometric data and atmospheric parameters

HD	$b-y$	m_1	c_1	β	Gr	$E(b-y)$	$T_{\rm eff}$ MD	$\log g$ MD	$T_{\rm eff}$ Gen	$\log g$ Gen	Broad	π mas	$\frac{\sigma_\pi}{\pi}$	M_v	σ	HIP
3003	0.014	0.179	0.991	2.910	5	−0.01	9340	4.38	9231	4.19	84	21.52	0.02	1.74	0.05	2578
4065	−0.019	0.153	0.909	2.865	1	0.00	10550	4.28	10242	4.16	30	7.55	0.16	0.44	0.35	3356
4150	0.012	0.133	1.090	2.858	1	0.02	9810	3.71			130	13.57	0.04	−0.06	0.09	3405
7916	0.036	0.150	0.967	2.870	5	0.04	9830	4.17			200	9.69	0.06	0.99	0.13	5992
15004	0.007	0.109	1.065	2.786	1	0.02	10220	3.29			200	5.05	0.21	−0.23	0.46	11261
15646	−0.014	0.150	1.027	2.889	5	0.00	10020	4.13	9974	4.08	50	8.47	0.06	0.99	0.14	11479
16152	0.007	0.173	0.995	–	5	−0.01	9510	4.36	9598	4.24	200	8.15	0.11	1.67	0.24	12055
17864	0.015	0.169	1.006	2.894	5	0.00	9420	4.23	9174	4.02	200	10.02	0.08	1.37	0.17	13271
18735	0.001	0.159	1.067	2.899	5	0.00	9590	4.09	9464	4.00	170	7.90	0.08	0.80	0.17	13947
20980	−0.001	0.165	1.042	2.916	5	0.00	9590	4.29	9431	4.18	30	7.25	0.10	0.66	0.22	15700
21473	0.022	0.170	1.110	2.895	5	0.01	9070	3.93	8895	3.90	50	7.39	0.07	0.63	0.16	16015
22789	−0.020	0.141	1.068	2.858	1	−0.01	10110	3.76	9881	3.87	100	7.81	0.09	0.47	0.21	17007
27660									8594	3.40	200	6.54	0.13	0.48	0.28	20360
30397	0.001	0.151	1.088	2.896	5	0.01	9700	4.01	9286	3.84	50	4.67	0.14	0.15	0.30	22136
31295	0.044	0.178	1.007	2.898	5	0.01	8970	4.25	8763	4.18	100	27.04	0.03	1.76	0.08	22845
32996	−0.019	0.140	0.939	2.848	1	0.00	10520	4.05	10364	3.99	20	8.98	0.08	0.81	0.18	23777
34868	−0.017	0.141	1.043	2.880	5	0.00	10120	4.01	9983	3.87	100	7.31	0.08	0.30	0.18	24831
34968	−0.020	0.124	1.059	2.830	1	−0.01	10250	3.59	10160	3.67	70	7.11	0.09	−1.04	0.20	24927
36473	0.003	0.155	1.038	2.899	5	0.01	9740	4.18	9605	4.10	50	12.00	0.07	0.89	0.14	25853
38056	−0.020	0.143	0.965	2.864	1	0.00	10400	4.11	10358	4.07	200	7.55	0.07	0.74	0.16	26796
38206	−0.014	0.165	0.940	2.907	5	−0.01	10170	4.48	10174	4.36	30	14.45	0.05	1.53	0.11	26966
42301	−0.008	0.146	1.030	2.877	1	0.00	9990	4.02	9856	4.07	200 − 300	12.77	0.05	1.02	0.12	29150
42729	−0.009	0.127	1.131	2.847	1	0.00	9760	3.54	9702	3.61	30	4.83	0.13	−0.50	0.27	29347
42834	−0.006	0.123	1.113	2.833	1	0.00	9840	3.51	9670	3.61	150	4.92	0.10	−0.26	0.22	29304
45557	−0.011	0.166	1.031	2.890	5	−0.01	9850	4.12	9759	4.05	200	11.37	0.04	1.06	0.09	30463
47827	−0.016	0.145	1.009	2.860	1	0.00	10160	3.94	10009	3.89	30	5.31	0.12	−0.32	0.26	31859
56341	−0.007	0.141	1.087	2.867	1	0.00	9780	3.77	9597	3.75	30	3.58	0.19	−0.89	0.41	35132
60629	−0.014	0.169	0.966	2.906	5	−0.02	10070	4.42	9986	4.21	50	9.65	0.07	1.56	0.16	36837
63112	0.008	0.117	1.089	2.831	1	0.02	9990	3.55			10	3.39	0.22	−1.04	0.47	37951
63584	−0.014	0.135	1.013	2.870	5	0.00	10200	4.01	10226	4.07	20	8.09	0.06	0.70	0.13	37720
67725	0.024	0.110	1.131	2.804	1	0.03	9870	3.30			250	4.57	0.17	−0.57	0.37	39898
69589	0.006	0.155	1.039	2.900	5	0.01	9720	4.19	9481	4.05	100	5.37	0.14	0.21	0.30	40561
71043	−0.001	0.157	1.014	2.918	5	0.00	9770	4.38	9575	4.23	200	13.68	0.03	1.57	0.08	41081
71155	−0.005	0.158	1.024	2.897	5	0.00	9780	4.20	9768	4.10	150	26.09	0.03	0.99	0.07	41307
71576	0.008	0.133	1.140	2.851	1	0.01	9600	3.55	9234	3.69	200	9.16	0.05	0.05	0.11	41003
74475	0.008	0.156	1.078	2.893	5	0.01	9570	4.01	9336	3.99	200	7.43	0.08	0.73	0.17	42775
76346	−0.011	0.143	0.973	2.881	1	0.00	10260	4.22	10190	4.14	200	11.01	0.04	1.22	0.09	43620
79108	−0.004	0.153	1.039	2.884	5	0.00	9830	4.05	9767	4.14	150	8.68	0.10	0.84	0.22	45167
80950	−0.014	0.165	0.934	2.910	5	−0.01	10180	4.50	10175	4.20	30	12.37	0.04	1.32	0.09	45585
84461	−0.025	0.140	1.045	2.865	1	−0.01	10290	3.88	10075	3.85	30	9.19	0.05	0.37	0.12	47717
85504	−0.017	0.137	1.040	2.840	1	0.00	10150	3.70	10259	4.01	20 − 30	3.11	0.31	−1.52	0.68	48414
87344	−0.024	0.123	0.905	2.779	1	0.00	10930	3.63	10725	3.71	30	6.83	0.26	0.47	0.57	49321
87363	0.005	0.178	1.029	2.902	5	−0.01	9440	4.22	9306	4.20	150	10.85	0.05	1.29	0.11	49259
87887	−0.006	0.125	1.082	2.829	1	0.01	9950	3.55	9913	3.73	20	11.35	0.10	−0.29	0.21	49641
92845	0.002	0.144	1.131	2.851	1	0.01	9550	3.56	9210	3.49	80	5.39	0.13	−0.76	0.28	52407
97585	−0.002	0.131	1.107	2.834	1	0.01	9780	3.52	9678	3.68	175	6.84	0.11	−0.47	0.24	54849
99922	0.030	0.162	1.033	2.905	5	0.02	9400	4.25			50	8.08	0.11	0.22	0.23	56078
101615	0.003	0.169	1.007	2.920	5	0.00	9580	4.41	9420	4.30	10	15.58	0.04	1.50	0.09	57013
104039	0.017	0.140	1.177	2.873	5	0.03	9580	3.60			≤10	3.66	0.19	−0.90	0.42	58436
104430	−0.006	0.148	1.005	2.895	5	0.01	10040	4.24	9816	4.04	50	10.56	0.07	1.23	0.14	58642
106797	0.007	0.166	0.906	2.885	1	0.00	9820	4.42	9674	4.18	150	9.72	0.06	1.00	0.13	59898
109573	0.006	0.157	0.986	2.926	5	0.01	9790	4.49	9774	4.30	150	14.91	0.05	1.61	0.11	61498
111519	0.017	0.153	1.099	2.899	5	0.02	9520	4.00			30	5.71	0.13	−0.05	0.28	62655
111786	0.161	0.131	0.805	2.773	1	0.00	7450	3.93	7397	4.29	10+150	16.62	0.04	2.25	0.09	62788
113852	0.006	0.178	1.035	2.911	5	−0.01	9400	4.27	9249	4.11	50	14.22	0.06	1.39	0.12	64003
114570	0.034	0.145	1.078	2.863	1	0.04	9710	3.78			250	11.45	0.05	1.03	0.12	64466
125473	−0.016	0.137	1.001	2.823	1	0.00	10270	3.68	9918	3.77	100 − 150	13.19	0.07	−0.35	0.14	70090
129791	0.034	0.139	0.969	2.872	5	0.04	10080	4.18			300	7.72	0.12	1.17	0.26	72192
139129	0.009	0.128	1.157	2.877	1	0.01	9560	3.67	9276	3.69	30	7.13	0.10	−0.35	0.22	76618
151527	0.172	0.067	1.079	2.793	6	0.05	7610	3.31			250	7.30	0.25	−0.13	0.53	82259
”					1	0.19	10130	3.47						0.47	0.53	”
152849	−0.005	0.141	0.995	2.864	1	0.01	10210	4.02	10030	4.07	200	8.99	0.15	0.29	0.32	82925
160263	0.008	0.116	1.126	2.827	1	0.02	9820	3.48			75	4.94	0.18	−0.83	0.40	86552
170680	0.006	0.140	1.052	2.892	5	0.02	9980	4.09			200	15.30	0.05	0.96	0.12	90806
188228	−0.008	0.145	0.959	2.897	5	0.01	10230	4.38	10146	4.28	100	30.73	0.02	1.36	0.04	98495
193571	−0.007	0.170	0.994	2.915	5	−0.01	9820	4.41	9652	4.25	80	13.35	0.06	1.22	0.13	100469
213320	−0.017	0.140	1.015	2.863	1	0.00	10200	3.95	10351	4.05	20 − 30	12.29	0.11	0.29	0.23	111123
213398	−0.004	0.167	1.045	2.910	5	−0.01	9640	4.24	9487	4.15	30	21.99	0.04	1.00	0.08	111188
216931									7558	4.06	50	11.76	0.07	1.95	0.14	113331
218639	0.005	0.152	1.037	2.884	5	0.01	9790	4.06	9391	4.06	200	9.45	0.11	1.26	0.23	114371
223352	−0.004	0.154	1.019	2.893	5	0.00	9860	4.19	9706	4.14	300	22.73	0.05	1.37	0.11	117452
225200	0.011	0.133	1.097	2.825	1	0.02	9780	3.51			300	7.75	0.12	0.74	0.26	345

When the value of the colour excess has been found to be negative, no correction has been applied to the colour indices $T_{\rm eff}$ and $\log g$.

3.3. $T_{\rm eff}$ and $\log g$ from Geneva photometry

We computed the atmospheric parameters from the Geneva photometric indices by using the recent calibration by Künzli et al. (1997).

This system provides an independent way to determine $T_{\rm eff}$ and $\log g$ since it does not include any filter centered on a Balmer line. We limited this computation to undereddened stars, i.e. to those which, according to $uvby\beta$ photometry, have a colour excess $E(b-y)$ in the range $\pm$ 0.01. The computed $T_{\rm eff}$ and $\log g$ are given in Table 2, Cols. 10 and 11.

3.4. Comparison of $T_{\rm eff}$ and $\log g$ values

The atmospheric parameters derived from the two photometric system are directly comparable only for stars with $E(b-y) = 0.0$. In order to have a larger sample, we consider as unreddened the stars with $E(b-y) \leq 0.01$ and, in order to have homogeneous data, the MD parameters have been recalculated for this comparison without taking into account the colour excess for stars with $E(b-y) = 0.01$.

Figures 1a and 1b display the results for $T_{\rm eff}$ and $\log g$ respectively; Fig. 1a does not include the abnormally low values of $T_{\rm eff}$ derived from both photometric systems for the λ Boo star HD 111786, which is, in fact, a binary, as demonstrated by Faraggiana et al. (1997).

We check the consistency of the two sets of $T_{\rm eff}$ and $\log g$ and we look for possible systematic differences. The values of $T_{\rm eff}$ from the $uvby\beta$ are systematically higher than those from the Geneva photometry. This difference is not related to the stellar rotation as it appears from the absence of any systematic relation between the $\Delta T_{\rm eff}$ and the $v \sin i$ value. Nevertheless, the difference between these two sets of values is small, the average being 150 K. The $\log g$ comparison shows higher scatter than that of $T_{\rm eff}$; the largest difference refers, to the already cited HD 111786. The star HD 85504, is an intriguing object with peculiar spectrum and kinematics (see the Appendix).

For most of the stars, $\log g$ (MD) is higher than $\log g$ (Gen) for large $\log g$ values, while the opposite is true for $\log g$ lower than 4. The correction of $\log g$ (MD) proposed by Napiwotzki et al. (1993), being independent of the $\log g$ value, does not solve this discrepancy.

A discrepancy between $\log g$ values obtained from these two sets of photometric indices, such as for HD 85504 and HD 111786 can be interpreted as a sign of difference in their flux distribution compared to that used for calibration. The H_β intensity plays an important role in the calibration of the Strömgren photometry, so we suggest that for these two stars, such a difference shows that their H_β intensity is not coherent with their continuum character.

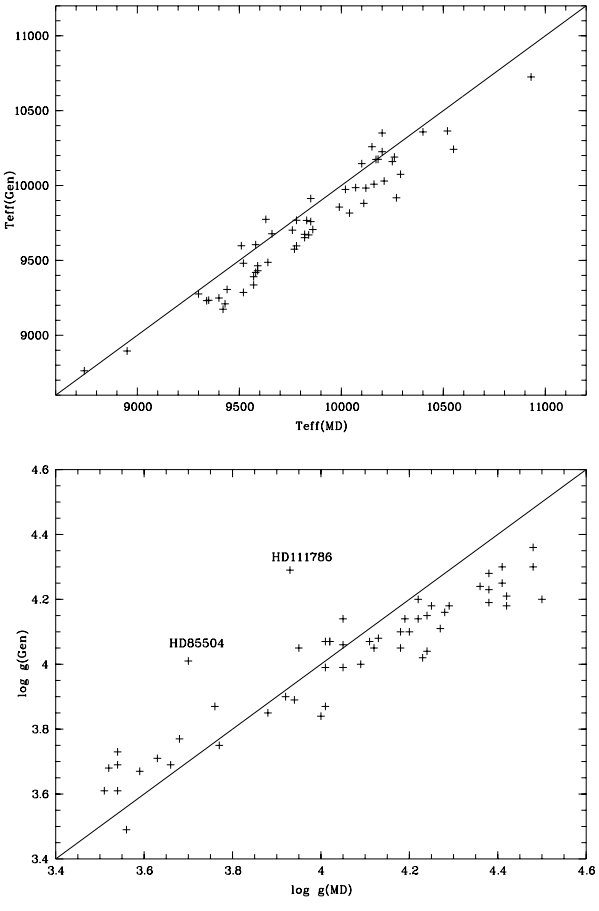

Fig. 1. Relation between $T_{\rm eff}$ (Fig. 1a) and $\log g$ (Fig. 1b) derived from MD and Geneva calibrations; no dereddening correction are applied to the colours in both systems, and only stars with $E(b-y) \leq 0.01$ are considered

Independently of the adopted calibration, it is clear that the A0 dwarf stars occupy a broad domain of $T_{\rm eff}$ and $\log g$ which leads to a loose correlation with spectral type and luminosity class appears. We remind that the internal accuracy reached by different MK classifiers is of $\pm$0.7 in luminosity class (Jaschek & Valbousquet 1997); the $\log g$ parameter plotted in Fig. 1b, cannot be directly related to this luminosity class.

If we exclude the binary HD 111786, the λ Boo star HD 31295 ($T_{\rm eff}$ (MD) = 8763 K) and the peculiarly reddened star HD 151527 ($T_{\rm eff}$(MD) = 7610 K), $T_{\rm eff}$(MD) spans from 9070 K (HD 21473) to 10930 K (HD 87344) and $\log g$ (MD), when only A0 V stars are considered, covers the range from 3.30 (HD 67725) to 4.50 (HD 80950).

4. Spectral analysis

The goal of this study is to establish an HR diagram for nearby A0 stars free of any peculiar object. The comparison between the observed spectra and those computed with the above derived parameters should allow to select the "normal" stars.

A grid of synthetic spectra, covering the range of the previously determined $T_{\rm eff}$ and $\log g$ values and based on Kurucz stellar model atmosphere (Kurucz 1993) has been constructed; solar abundances and a microturbulence value equal to 2 $\rm km\,s^{-1}$ are adopted. Computations have been made with various rotational broadening values for each synthetic spectrum.

From the grid of the Kurucz fluxes (1993) we computed also the UV fluxes in the four TD1 bands; the comparison between the observed and computed colour indices $m_{\rm UV-V}$ has been systematically done. The choice of these data is due to the fact that the Thompson et al. (1978) Catalogue contains all but 2 stars of our sample, while only 14 of them have been observed by IUE in the low resolution mode and have spectra available from the Final Archive.

In order to compare the optically observed spectra with the computed ones, the needed shift in wavelength to be applied to the observed spectrum is obtained by cross correlation. The templates used are the spectra computed with the appropriate stellar parameters. The cross correlation program differs from the Midas command XCORRELATE in the sense that the correlation index is normalized to 1. The template and the spectrum are rebinned in the velocity space, the rebinning being largely oversampled, the shift is applied and the spectrum rebinned back in wavelength at its original stepsize.

As by-product of this program, the correlation curve contains informations on the quality of the fit between observed and computed spectra.

The broadening parameter (Table 2, Col. 14) refers to the v sin i value adopted for the best fit of the observed and computed spectrum and, in the case of spectroscopic binaries, does not have any physical meaning.

The selection of the normal stars follows from the application of tests based on:

• *The correlation curve*
The height and the shape of the correlation curve are related to similarity of the synthetic spectrum and the observation; in particular, a non symmetric correlation curve indicates a possible binarity.

• *Coherence between MD and Geneva parameters*
The comparison between the MD and Geneva parameters for stars with $E(b-y) = 0.00$ shows that the largest difference in $T_{\rm eff}$ is 352 K (HD 125473), significantly larger than the uncertainties expected for the $T_{\rm eff}$ determination from errors on photometric colour indices. We note that for this star the MD parameters are those from which the best fit with the computed spectrum is obtained.

We remark that for several stars the $\log g$ computed by MD from Strömgren photometry is higher than what expected for dwarf A0 stars. We looked at the eleven stars with $\log g$ higher than 4.3 (HD 3003, HD 16152, HD 38206, HD 60629, HD 71043, HD 80950, HD 101615, HD 106797, HD 109573, HD 188228, HD 193571). None of them has an H_γ profile which fits the spectrum computed with the MD parameters. For all these stars $E(b-y) \leq 0.01$, so that the Geneva parameters are computed as well. The $\log g$ computed from the Geneva photometry is systematically lower and the spectrum computed with Geneva parameters from undereddened colours, fits better the H_γ profile.

• *Observed and computed profiles*
The core of the observed H_γ is expected to be deeper than that computed for the appropriate v sin i value with Kurucz models which do not include NLTE effects; therefore an observed profile shallower than the computed one is a sign of abnormality. In highly rotating stars Mg II 4481 is the only metallic feature with a measurable profile; this feature is expected to be rotationally broadened, as soon as the 0.02 Å separation of the Mg II doublet becomes irrelevant compared to the stellar v sin i value.

5. Spectroscopic behaviour of double stars

According to the values given Table 1 Cols. 5 and 6 we can suspect that the photometric indices and consequently the derived atmospheric parameters, are affected by a companion for 10 stars. The Δm and the angular separation is such that the spectra of five of these binaries must be composite: HD 3003, HD 4065, HD 47827, HD 104039, HD 152849.

According to our analysis of the spectra we note:

• HD 3003: The correlation curve is not symmetric and the Mg II 4481 is not rotationally broadened (Figs. 2a and b).

• HD 4065: The profile of H_γ is not fitted by the computed ones with MD or Geneva parameters and the core of the line is considerably shallower than the computed ones (Figs. 3a and b); the Mg II 4481 has a very peculiar profile and the metal lines are poorly reproduced by computations (Fig. 3c).

• HD 47827: The Mg II profile has broad wings as in the previous star; H_γ is slightly asymmetric and flatter than the computed one and the metallic lines are too weak for a non peculiar star.

• HD 104039: The duplicity is dubious according to the Remarks in the BSC. This star has $E(b-y) = 0.03$

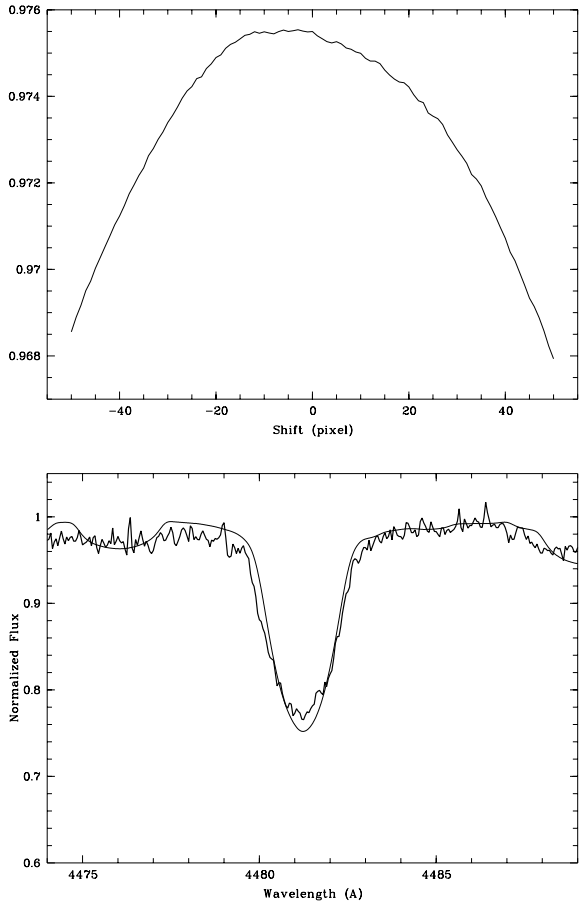

Fig. 2. a) the cross correlation between the observed spectrum of HD 3003 and the computed one (1 pixel = 0.05 Å). **b)** the Mg II 4481 line (thick line) overplotted on the computed one (thin line)

as HD 7916 (see below). H_γ does not fit the synthetic spectrum computed with the MD parameters taking into account the reddening; the metal lines are stronger than the computed ones. A better fit is obtained with the spectrum computed with the parameters corresponding to no colour excess, but the metal lines intensities do not agree even with these parameters; also the TD1 colour indices fit better those computed with no colour excess.

• HD 152849: The spectrum is of low S/N quality and the line profiles cannot be as well defined as in most of the other spectra but the profile of Mg II 4481 is non rotationally broadened (Fig. 4) and we have checked that this conclusion does not rely upon the position of the continuum.

We conclude that, at the resolution of our spectra, the contamination by a companion star can be detected by at least one of the criteria we have chosen:

a) non symmetry of the cross correlation curve (see Fig. 2a)

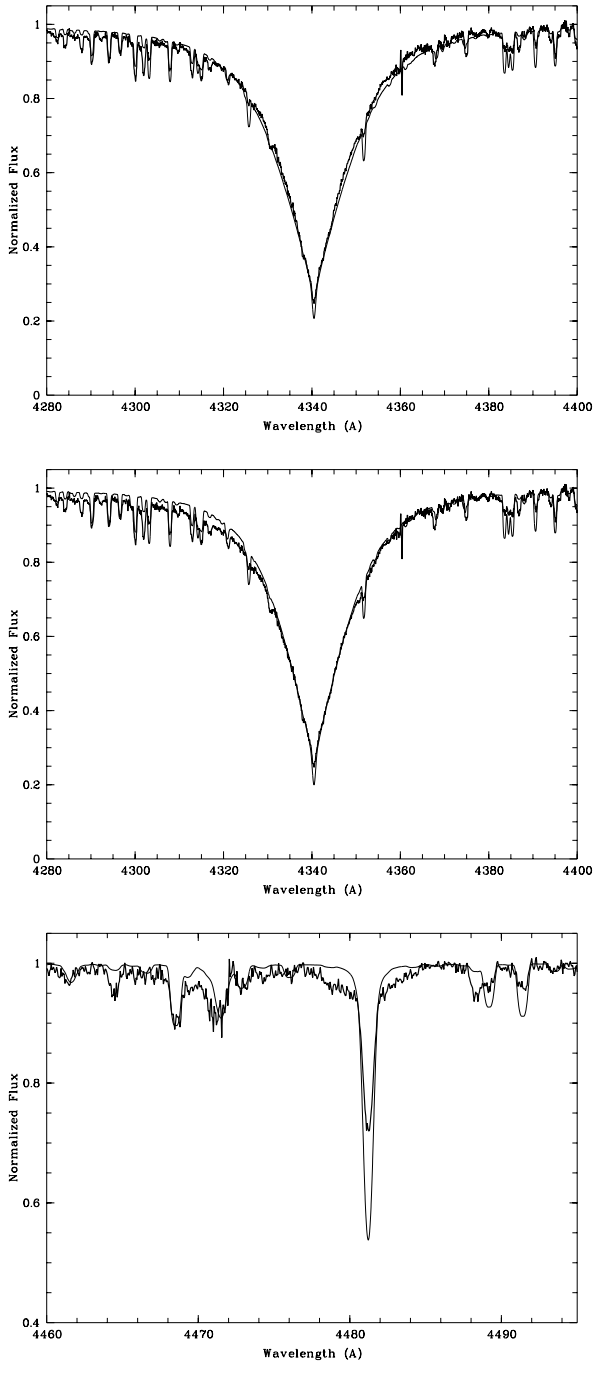

Fig. 3. a) the observed H_γ (thick line) of HD 4065 overplotted on that computed with MD parameters. **b)** the same, but with Geneva parameters. **c)** the Mg II 4481 region compared with the computed spectrum (at λ4470 a defect of the CCD is present)

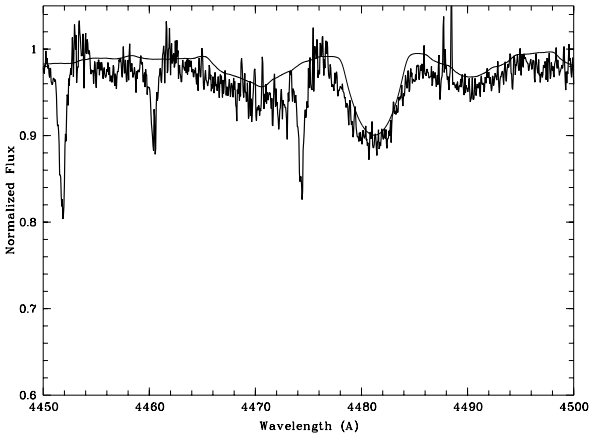

Fig. 4. The Mg II 4481 region of HD 152849 (thick line) compared with the computed spectrum (thin line); the narrow features at $\lambda\lambda$4452, 4460 and 4473 correspond to defects of the CCD

b) peculiar profile of Mg II 4481 line (see Figs. 2b, 3c, 4)

c) distorted line profiles and/or flat H_γ core (see Fig. 3a).

In this temperature range the H_γ line is so strong that the cross correlation is dominated by its profile; if the combined profile of a binary star can be reproduced by a model, the duplicity detection is confined to the behaviour of the metal lines.

For the other 5 binaries, HD 7916, HD 17864, HD 34968, HD 99922, HD 213320, the Δm and/or their separation are such that, a priori, their spectra will not be affected by the companion. Nevertheless, we found some peculiarities in their spectra.

• For HD 7916 the Mg II 4481 is broader than the other metal lines and we found indications of duplicity in the line profiles; the profiles of H_γ and Mg II 4481 (Figs. 5a and b) indicate the presence of a secondary companion on the short wavelength side and these peculiarities cannot be due to the visual companion which has a too faint magnitude according to the Δm given in Table 1; however a lower magnitude difference, $\Delta V = 1.95$ has been measured by the Hipparcos experiment in good agreement with the value (1.84), estimated by Corbally (1984). We note that HD 7916 is one of the most reddened stars; we interpret this colour excess as an ad hoc quantity needed to reproduce the colours of a single normal star.

• For HD 17864 The Mg II profile is peculiar: flat and its broadening does not correspond to a rotational broadening. The H_γ profile is asymmetric with a too flat core.

• For HD 99922 the magnitude difference and the separation are too large to affect our spectroscopic data; unfortunately, the Mg II 4481 region is not available on our spectrum. Neverthless we note that the other metal lines are abnormally shallow and weak and strongly suggest a

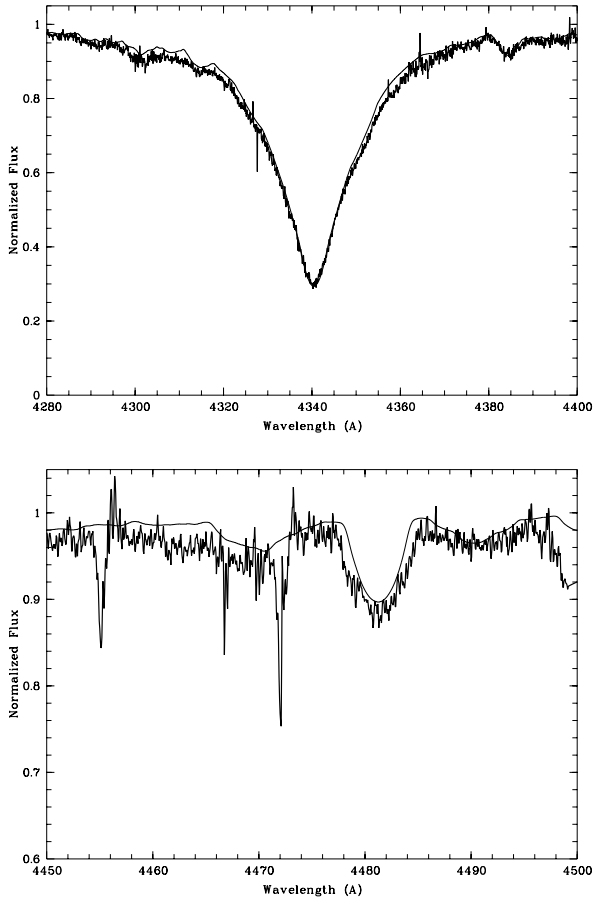

Fig. 5. The observed and computed spectra of HD 7916 in the regions of H_γ (Fig. 5a) and Mg II 4481 (Fig. 5b); sharp and narrow absorptions are due to bad CCD columns

"veiling" effect (Fig. 6), according to the definition introduced by Corbally (1987). We interpret these peculiarities as due to a source which cannot be identified with the known companion.

• In the spectrum of HD 34968 only a slight asymmetry of the MgII line profile is detected.

• For HD 213320 the H_γ profile is very well reproduced by computations; in spite of this, the metallic lines present distorted profiles and their intensity is poorly reproduced by the synthetic spectrum.

So we note that unexpectedly distorted line profiles are found also among these 5 stars.

6. Search for reference stars

Using the criteria listed above, we extend a similar analysis to all the sample stars. The results are summarized in Table 3.

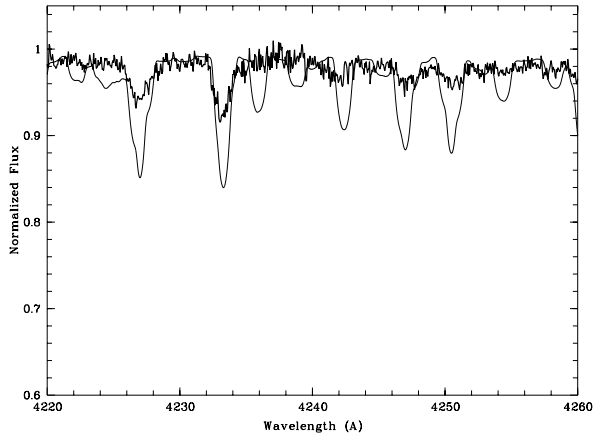

Fig. 6. The observed (thick line) and the computed (thin line) spectra of HD 99922 shown a pronounced "veiling" effect on the metal lines

From this analysis it appears that a large percentage of our sample stars (being either binaries or peculiar) cannot be used to build a set of reference stars.

6.1. Newly detected binaries

For 13 stars the cross correlation curve has a highly distorted shape (see, for example, the cross correlations of HD 36473 and HD 56341 in Figs. 7a and b). In all the spectra of these stars the line profiles are distorted; details on each star are summarized in Table 3 and in the Appendix.

These stars are:
HD 16152, HD 21473, HD 22789, HD 30397, HD 36473, HD 56341, HD 104430, HD 106797, HD 111519, HD 111786, HD 113852, HD 139129, HD 151527.

HD 111786 has been discussed by Faraggiana et al. (1997) and its highly distorted UV colours are plotted in Fig. 8b.

HD 139129 is the only star for which spectroscopic informations are found in the literature (see Appendix); the peculiar abundances, derived by Lemke (1989, 1990), strengthen our binary interpretation.

HD 151527 is an abnormally reddened star; the choice of the Strömgren group according to the lowest value of the colour excess produces atmospheric parameters in conflict with observations; from $E(b-y) = 0.19$ the derived atmospheric parameters produce a synthetic spectrum which agrees with observed H_γ, but not with the metal lines spectrum. We note also the low value of the derived $\log g$ value, in disagreement with its MK classification. The distorted UV colours of this star are plotted Fig. 8c; this star and HD 111786 are the only two objects for which a large discrepancy between observed and computed UV colours is found.

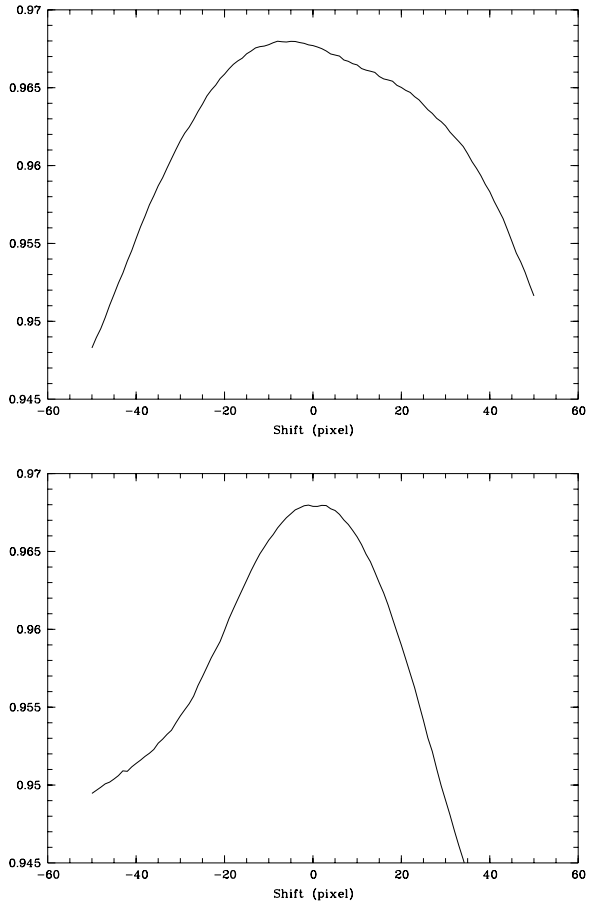

Fig. 7. The distorted cross correlations of HD 36473 **a)** and of HD 56341 **b)** indicate the presence of a secondary shifted source. (1 pixel = 0.05 Å)

According to the Hipparcos and Tycho Catalogues (ESA, 1997) HD 111519, HD 113852 and HD 151527 are probable astrometric binaries, due to the flag in field 59 of the Hipparcos Catalogue.

6.2. Suspected binaries

For other stars, even if the cross correlation is not as distorted as for the previous ones, the spectral peculiarities and the distorted line profiles suggest a binary nature of the observed objects or some peculiarity.

The 9 stars suspected to be binaries on the basis of the visual and UV data are: HD 15646, HD 20980, HD 71043, HD 79108 HD 84461, HD 114570, HD 129791 HD 188228 and HD 193571. Details on them can be found in Table 3 and in the Appendix.

We note that HD 188228 belongs to the system of standard stars for rotational velocity determinations defined by Slettebak et al. (1975); the $v \sin i$ value derived by Levato (1972) differs considerably from that by Slettebak et al.

Table 3. Summary of the spectral analysis

HD	cross corr.	H_γ	Mg II	metal lines	Comments
3003	not symm.	–	not rot.	–	
4065	–	syn. deeper	broad + sharp	–	
4150	–	–	–	–	
7916	–	double core	double	–	
15004	–	shell	not rot.	shell	shell star
15646	flat	–	slight asymm.	–	SrII/ScII > 1
16152	not symm.	poor fit	poor fit	–	on 13/Nov./92
	–	poor fit	–	–	on 14/Nov./92
17864	–	poor fit	not rot.	–	
18735	–	–	poor fit	–	
20980	flat	–	strong	poor fit for some	
21473	not symm.	poor fit	poor fit	poor fit	
22789	not symm.	poor fit	not rot.	–	
27660	–	–	–	–	
30397	not symm.	–	red wing	some flat	
31295	–	syn. deeper	–	–	
32996	–	–	–	–	SrII/ScII > 1
34868	–	–	–	–	
34968	–	–	slight asymm.	–	
36473	flat and asymm.	poor fit	not rot. + flat core	some flat	
38056	–	–	–	–	
38206	–	–	–	some lines flat and weak	
42301	–	–	–	–	
42729	not symm.	–	–	many lines flat and weak	
42834	–	–	–	–	
45557	–	–	not rot.	–	
47827	–	syn. deeper	broad + narrow	weak	
56341	not symm.	double peak	two components	flat and weak	SB2
60629	–	–	–	–	H_γ fits with Gen param.; SrII/ScII > 1
63112	–	–	–	–	ScII + some lines weak
63584	–	–	–	–	SrII/ScII > 1
67725	–	poor fit	–	–	higher $\log g$ required
69589	–	–	not rot.	some weak	H_γ good fit with Gen param.
71043	–	–	asymm.	–	
71155	–	–	slight asymm.	some flat core	
71576	–	slight asymm.	strong and not rot.	–	
74475	–	–	strong	–	
76346	–	–	not rot.	–	
79108	–	–	not rot.	flat and weak	
80950	not symm.	–	–	some weak	
84461	–	–	not rot.	flat core	MD param. do not fit well
85504	–	–	pec. wings	some lines strong	Gen param. fit better
87344	–	–	–	some weak	
87363	–	–	–	–	
87887	–	–	–	–	
92845	–	–	–	–	
97585	–	–	strong	–	
99922	===	–	===	very weak	only half range covered
101615	–	–	–	some weak lines	
104039	–	poor fit	poor fit	poor fit	
104430	flat	poor fit	not rot.	flat and weak	
106797	very asymm.	very bad fit	asymm.	poor fit	
109573	–	–	–	flat and weak	H_γ fits Gen param.; β Pic star
111519	flat	poor fit and syn. too deep	narrow + broad	very weak	
111786	two peaks	very poor fit	very weak	narrow + broad	abnormal TD1 color indices
113852	not symm.	asymm.	not rot.	poor fit	SrII/ScII > 1
114570	–	slight narrow core	–	–	
125473	–	–	–	–	
129791	–	–	not rot.	some narrow lines	
139129	not symm.	–	not rot.	very weak	
151527	slight asymm.	narrow core	very bad fit	bad fit	$T_{\rm eff}$ = 10000
		very bad fit	very bad fit	very bad fit	$T_{\rm eff}$ = 7500, bad fit for H_γ, TD1 distorted
152849	–	–	not rot.	–	
160263	–	–	pec cor	some weak	
170680	–	–	weak	weak	λ Boo star
188228	–	–	poor fit	poor fit	
193571	not symm.	–	slight asymm.	–	
213320	–	–	–	poor fit	SrII/ScII > 1
213398	–	–	–	–	
216931	not symm.	–	very broad	poor fit	bad classification $T_{\rm eff} \simeq 8000$
218639	–	–	–	–	
223352	–	–	–	–	
225200	–	shell core	–	some shell profiles	shell star

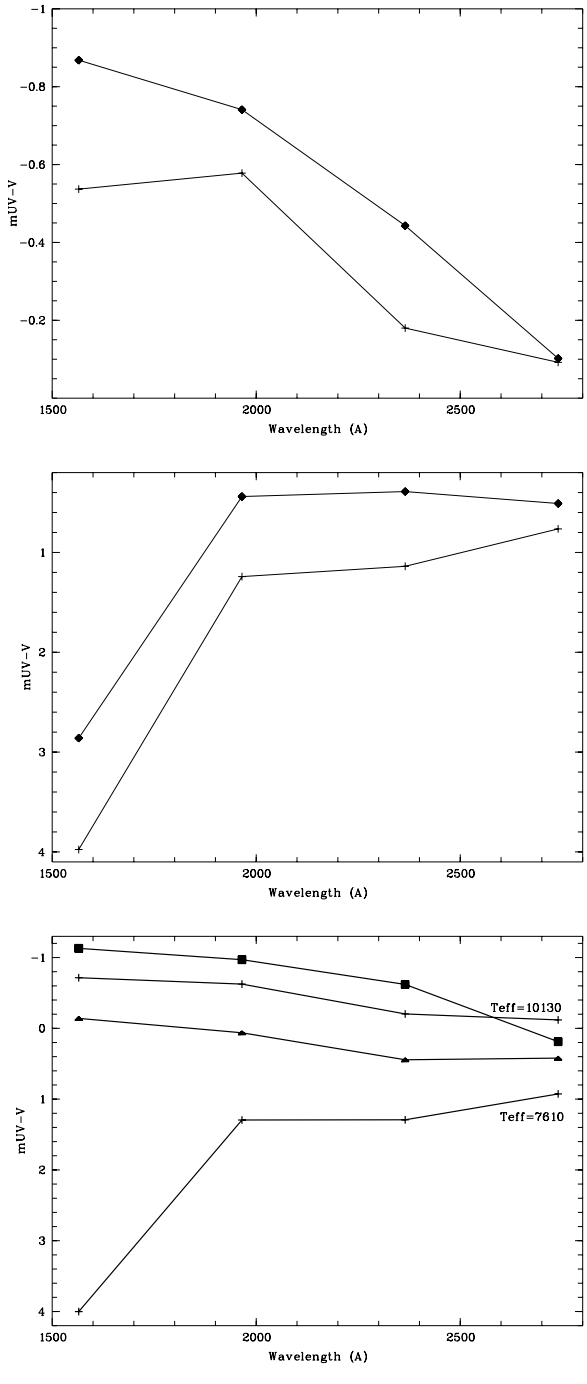

Fig. 8. The observed UV colour indices $m_{\rm UV} - V$ dereddened according to the $E(b-y)$ given in Table 2 and compared with those computed with the MD atmospheric parameters for **a)** HD 109573, **b)** HD 111786 and **c)** HD 151527 where the filled triangle refer to $E(b-y) = 0.05$ and filled square to $E(b-y) = 0.19$. The computed values are indicated with (+). (see comments on HD 109573 in the Appendix)

For HD 129791, in the Hipparcos Catalogue (ESA, 1997), a note in the field 59 indicates that it is probably an astrometric binary.

6.3. Remarks from Hipparcos astrometric data

In the Hipparcos Catalogue (ESA, 1997) besides the stars for which a companion is observed and its motion described, there are several stars from Table 1 considered as probable astrometric binaries on the basis of their astrometric solution.

They are: HD 4150, HD 42301, HD 63584, HD 87887, HD 92845, HD 109573 HD 111519, HD 113852, HD 129791, HD 151527, HD 223352.

Among these 11 stars only 4 present spectral peculiarities indicating a possible binarity. We cannot expect to have a one to one coincidence because the detection of binarity indices in the spectra at our disposal requires a small difference in magnitude and separation, and a difference in radial velocity if the two components have similar rotational velocities.

The other peculiar objects are:

6.4. Shell stars

HD 225200 is a shell star; its spectrum is similar to that of the already known shell star HD 15004. The hypothesis of binarity for HD 225200, as suggested by AM, must be rejected because the sharp components are only present on the lines expected in shell stars: the core of H_γ, all the strong lines of the Fe II Multiplet 27 and the Ti II 4468.

6.5. A misclassified star

HD 216931 has been misclassified as A0, according to our two spectra; these two spectra refer to an object much cooler than an A0 star. The parameters given in Table 2 have been derived from the Geneva photometry, neglecting any colour excess, in spite of the $E(B-V) = 0.06$. The whole spectrum (and in particular the H_γ profile) is not reproduced by that computed with the above parameters. The H_γ profile is fitted by a spectrum computed with a temperature 500 K higher than the predicted one, (so that the neglected reddening can be at the origin) i.e. by the spectrum computed with $T_{\rm eff} = 8000$ K and $\log g = 4.0$, values which produce a fairly good agreement also between observed and computed UV colours. However several metal lines are poorly fitted by the synthetic spectrum computed with these parameters; the ratio SrII4215/ScII4247 of the observed spectrum is much higher than the computed one, as in Am stars; several stronger than computed features are present on the two

observed spectra. The Mg II 4481 is distorted and very broad compared to other metal lines.

The presence of a companion which cannot be identified with the known B and C components of this visual triple system (ADS 16392) is reported by Richichi et al. (1997) from lunar occultations observed in the near infrared and must be at the origin of the observed peculiarities and of the discrepancy between our two spectra and the MK classification.

7. Results of the search for reference stars

7.1. Remarks on cross correlation

The cross correlation shape is highly dominated by the strong H_γ line which cannot be recorded, at high resolution, on a single order of an echelle spectrograph. Even if great care has been taken in connecting the orders and on the normalization procedures, a doubt remains on the reliability of H_γ profile, since the continum between the very broad wings has been placed by connecting them with a straight line.

The possibility that instrumental effects are not totally eliminated by the Flat Field correction cannot be discarded, the light path not being the same for the star and for the tungsten lamp. Consequently, it remains a possible source of some of the slight asymmetries of H_γ profiles and of the cross correlation shape which is dominated by the effect of this strong line profile.

7.2. Remarks on colour excess

There are 7 stars (HD 7916, HD 67725, HD 104039, HD 114570, HD 129791, HD 151527, HD 216931) for which $E(b-y)$ is higher than 0.02. For all, but HD 67725, spectral peculiarities have been detected (see previous section); for HD 67725 we note that the $\log g$ value derived from the colours is abnormally low for an A0 V star and the corresponding computed H_γ does not fit the observed one.

So all the reddened stars present some spectral peculiarity.

7.3. Remarks on hot Am detection

Among the CP stars the strong lines of Si II and Mn II lie out of our observed spectral range so preventing us to detect hot Ap stars.

We can detect the Am character through one of the classical criteria, the SrII4215/ScII4247 ratio higher than that expected for solar abundances. According to this criterium, the mild hot Am candidates are: HD 32996, HD 63584 and 213320.

We note also that for two suspected binaries, (see Table 3), HD 15646 and HD 113852, the ratio SrII 4215/ScII 4247 is much higher than that expected for solar abundances. A spectral classification based only on this ratio may wrongly assign to the Am class an object that is, in reality, a spectroscopic binary whose components do not differ much in luminosity. This may be the case for HD 60629; several metal lines show an abnormal core.

7.4. Reference stars

We conclude that from our original sample of 71 stars at least 21 (the 8 out of the 10 stars discussed in Sect. 5 (i.e. all, but HD 34968 and HD 213320) and the 13 stars discussed in Sect. 6.1) cannot be considered as reference stars, so that the masses and ages are computed for a reduced sample of 50 stars only.

However, doubts remain on other stars, due to possible binarity as indicated in Sect. 6.2; for several of the remaining stars the peculiarities are not strong enough to exclude any instrumental origin; however, a significant reddening remains difficult to accept for such nearby stars, large discrepancies between results obtained by other authors on $v \sin i$ (e.g. the discrepant results found for HD 4150) and more subtle discrepancies as those discussed in the Appendix, suggest that the number of binaries and/or peculiar objects may be higher than that selected in this section.

High rotation is expected to affect the photometric colours (Collins & Smith 1985) and the line intensities (Slettebak et al. 1980) of A-type stars. The weakening of Hgamma and Mg II 4481 lines due to rotation is computed in the latter paper; we could not reveal any correlation between the intensities of these lines and the $v \sin i$ values, the rotational effect being probably masked either by the unknown i value and/or by the fact that most of the non binary stars of our sample have $v \sin i$ lower than 200 km s^{-1}. Also a relation between the spread on the HR diagram (see next section) and the stellar vsini has been searched, but not detected. In particular no trend between $\log g$ and $v \sin i$ appears, nor are the oldest stars those with lower $v \sin i$.

8. Mass and age of dwarf A0 stars

8.1. The HR diagram

Hipparcos parallaxes enable us to establish the HR diagram for this set of stars, in order to determine their masses and ages.

The effective temperature is that derived from photometric calibrations. The visual absolute magnitudes

Table 4. Parameters computed from the HR diagram and evolutionary tracks for the reduced sample; the star HD 216931 has been excluded from this table as well as HD 27660. The evolutionary tracks used for these computations are those by Schaller et al. (1990). The errors are given for the determination of $\log(L/L_\odot)$, $\mathcal{M}/\mathcal{M}_\odot$, $\log g_{\rm ev}$. For the ages the error is given in percentage

HD	$\log(L/L_\odot)$	σ	$\mathcal{M}/\mathcal{M}_\odot$	σ	$R/R_\odot$	$\log g_{\rm ev}$	σ	Age (log(yrs))	σ (%)	HIP
4150	2.01	0.04	2.82	0.07	3.52	3.80	0.03	8.51	7	3405
15004	2.11	0.18	2.98	0.24	3.64	3.79	0.14	8.45	11	11261
15646	1.60	0.06	2.40	0.08	2.11	4.17	0.05	8.42	34	11479
18735	1.65	0.07	2.39	0.09	2.43	4.05	0.06	8.57	17	13947
20980	1.71	0.09	2.45	0.10	2.59	4.00	0.07	8.58	13	15700
31295	1.22	0.03	1.97	0.07	1.69	4.28	0.03	8.42	70	22845
32996	1.72	0.07	2.56	0.09	2.19	4.17	0.06	8.34	37	23777
34868	1.89	0.07	2.70	0.10	2.88	3.95	0.06	8.49	11	24831
34968	2.44	0.08	3.47	0.15	5.27	3.54	0.07	8.35	10	24927
38056	1.74	0.06	2.57	0.09	2.29	4.13	0.05	8.40	27	26796
38206	1.45	0.05	2.29	0.10	1.72	4.33	0.03	6.95	157	26966
42301	1.59	0.05	2.38	0.08	2.09	4.18	0.04	8.42	34	29150
42834	2.09	0.09	2.93	0.13	3.84	3.74	0.07	8.48	8	29304
42729	2.19	0.11	3.05	0.16	4.34	3.65	0.09	8.46	13	29347
45557	1.57	0.04	2.34	0.07	2.09	4.17	0.04	8.45	33	30463
60629	1.43	0.06	2.26	0.10	1.71	4.33	0.04	6.97	162	36837
63584	1.74	0.05	2.54	0.08	2.37	4.09	0.05	8.45	22	37720
63112	2.42	0.19	3.25	0.25	5.41	3.49	0.15	8.42	15	37951
67725	2.22	0.15	3.11	0.20	4.41	3.64	0.12	8.44	14	39898
69589	1.90	0.12	2.67	0.15	3.14	3.87	0.10	8.54	10	40561
71576	1.95	0.05	2.73	0.08	3.43	3.81	0.04	8.54	8	41003
71043	1.36	0.03	2.17	0.09	1.68	4.33	0.03	7.05	120	41081
71155	1.59	0.03	2.36	0.06	2.18	4.14	0.03	8.49	24	41307
74475	1.68	0.07	2.42	0.09	2.51	4.02	0.06	8.58	15	42775
76346	1.53	0.04	2.37	0.08	1.86	4.28	0.01	8.14	71	43620
79108	1.65	0.09	2.42	0.10	2.32	4.09	0.07	8.51	24	45167
80950	1.49	0.04	2.32	0.08	1.78	4.30	0.03	7.90	91	45585
84461	1.88	0.05	2.70	0.08	2.74	3.99	0.04	8.47	12	47717
85504	2.62	0.27	3.62	0.46	6.63	3.35	0.20	8.31	26	48414
87363	1.44	0.05	2.19	0.07	1.98	4.19	0.04	8.50	34	49259
87344	1.89	0.23	2.78	0.24	2.46	4.10	0.16	8.34	47	49321
87887	2.11	0.08	2.96	0.12	3.83	3.74	0.07	8.47	8	49641
92845	2.27	0.11	3.16	0.17	5.00	3.54	0.10	8.45	12	52407
97585	2.17	0.10	3.03	0.16	4.26	3.66	0.08	8.47	13	54849
101615	1.37	0.04	2.15	0.08	1.76	4.28	0.03	8.26	78	57013
109573	1.37	0.04	2.18	0.10	1.68	4.33	0.03	7.05	126	61498
114570	1.57	0.05	2.33	0.08	2.16	4.14	0.04	8.50	28	64466
125473	2.17	0.06	3.06	0.10	3.84	3.76	0.04	8.43	7	70090
129791	1.54	0.11	2.35	0.11	1.93	4.24	0.07	8.30	62	72192
160263	2.32	0.16	3.25	0.20	5.02	3.55	0.12	8.41	13	86552
170680	1.62	0.05	2.40	0.08	2.15	4.15	0.04	8.44	29	90806
188228	1.48	0.02	2.31	0.09	1.74	4.32	0.02	7.43	111	98495
193571	1.50	0.05	2.28	0.07	1.94	4.22	0.04	8.39	51	100469
213320	1.90	0.09	2.72	0.12	2.87	3.96	0.07	8.48	12	111123
213398	1.57	0.03	2.33	0.07	2.20	4.12	0.03	8.53	23	111188
218639	1.48	0.09	2.27	0.09	1.92	4.23	0.07	8.37	60	114371
223352	1.44	0.04	2.24	0.08	1.81	4.27	0.03	8.23	81	117452
225200	1.69	0.10	2.45	0.11	2.44	4.05	0.08	8.53	21	345

(M_V) and their σ are computed from the parallax data taken from the Hipparcos Main Catalogue and given in Cols. 13, 14 and 15, 16 of Table 2. These values are obtained by taking into account the colour excess.

One of our goals being to compute the stellar masses, we restrict the analysis to the reduced sample defined in the previous section.

We create the HR diagram by plotting the $T_{\rm eff}$ derived from the MD calibration versus the luminosity (Fig. 9). The luminosity has been computed from M_V with a bolometric correction taken from the Bessell et al. (1998) tables and $M_{\rm bol\odot} = 4.75$, as given by Cayrel de Strobel (1996), and adopted by IAU Commissions 29 and 36 (1997, IAU General Assembly). The values of $L/L_\odot$ are given in Table 4, Col. 2 and the errors in Col. 3; these latters are due to the errors on the parallaxes. On this plot the stars are divided according to their photometrically derived $\log g$(MD) values. The evolutionary tracks by Schaller et al. (1992) are overplotted for 2.0, 2.5 and 3.0 solar masses, and $Z = 0.02$.

The cross represents the Vega position ($T_{\rm eff}$ = 9550 K; log g = 3.95 according to Castelli & Kurucz (1994). The position of the misclassified HD 216931 lies out of the boundaries of the plot.

We note the large spread in luminosity; we note also that Vega parameters do not represent the average values of dwarf A0 stars neither in luminosity nor in $T_{\rm eff}$.

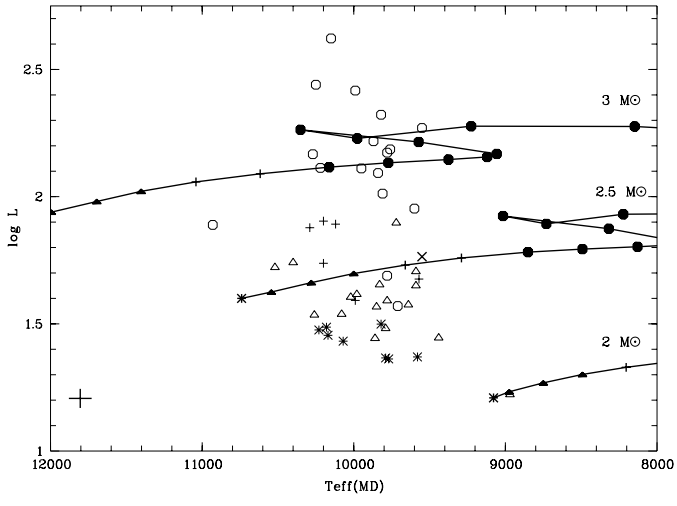

Fig. 9. The HR diagram for the reduced sample. The luminosity is expressed in $L/L_{\odot}$. The $\log g$ ranges are distinguished by using the following symbols: $*$ $\log g \geq 4.3$; $\triangle$ $4.05 \leq \log g$ <4.3; + $3.8 < \log g < 4.05$; hexagone $\log g \leq 3.8$; The filled symbols triangle and hexagone are used for the evolutionary tracks with the same intervals for $\log g$. Vega is labelled with the symbol: $\times$

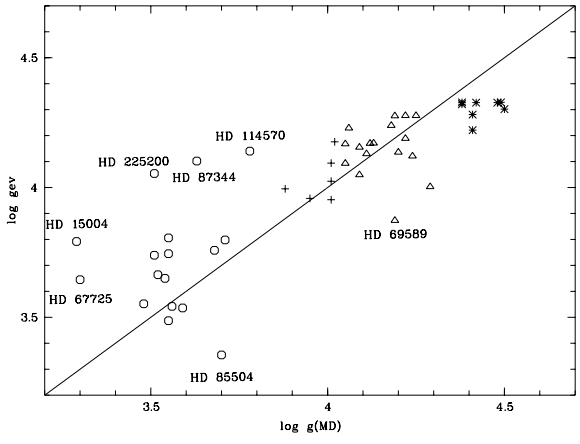

Fig. 10. The relation between $(\log g)_{\rm ev}$ and $(\log g)_{\rm ph}$; the latter is that derived from the MD calibration; the symbols are the same as in Fig. 9

We remark that the only non peculiar A0 III star of our sample (HD 87887) does not have the lowest $\log g$ value (3.55), nor the brightest luminosity ($\log(L/L_{\odot}) = 2.11$). If we do not consider the shell stars, the most extreme values, which should indicate the most luminous objects, are the lowest value of $\log g = 3.30$ (HD 67725) or the largest value for $\log(L/L_{\odot})$ (2.62) (HD 85504); we note that both refer to stars classified as A0 V.

We recall that HD 67725 ($\log(L/L_{\odot}) = 2.22$) is reddened and has an H_{γ} profile which is not reproduced by computations. HD 85504 is a peculiar object which has the spectral properties of a Population I star and the kinematics of a Population II star, according to Adelman & Pintado (1997).

8.2. Evolutionary based surface gravity

We used the HR diagram to derive the value of $\log g_{\rm ev}$ from evolutionary models and the Hipparcos parallaxes in order to compare them with the value of $\log g_{\rm ph}$ obtained from photometric data.

Balona (1994) found serious discrepancies between the gravities derived from evolutionary models and those obtained from photometric and spectroscopic determinations; this author questioned the reliability of the photometrically derived $\log g$ values and of the Kurucz (1979) LTE grid of models.

To compute $\log g_{\rm ev}$ ($g_{\rm ev} = {\rm G}\mathcal{M}/R^2$), we applied the following relation:

$R = (L/4\pi\sigma T_{\rm eff}^4)^{1/2}$

The stellar masses $\mathcal{M}/\mathcal{M}_{\odot}$ are derived from $L/L_{\odot}$ and $T_{\rm eff}$ by interpolation using Asiain (1998) method on the same evolutionary tracks (Schaller et al. 1992) used in the previous sub-section. The results are given in Table 4 Col. 4 and Col. 5 for the errors; the mean value of the error on the mass determination, due to the uncertainty on M_V is 0.1 $\mathcal{M}/\mathcal{M}_{\odot}$.

We compare these $\log g_{\rm ev}$ (the values are given Table 4) with the $\log g_{\rm ph}$ obtained from *ubvyβ* photometric data Fig. 10. The $\log g_{\rm ph}$ have been already compared with model atmosphere calculations; our data include a Balmer line, which in this domain of temperature, is highly sensitive to the surface gravity. If we exclude the two shell stars (HD 15004, HD 225200) the most discrepent between the two $\log g$ determinations are for: HD 67725, HD 85504, HD 114570 whose peculiarities are discussed in the Appendix; for two more stars, HD 69589 and HD 87344, we do not have any obvious explanation.

From the diagram plotted Fig. 10 we note that, for most of the stars, the evolutionary gravities agree reasonably well with the photometric ones, the $\log g_{\rm ev}$ being systematically slightly higher than the $\log g_{\rm ph}$, except for the stars with $\log g \geq 4.3$. The behaviour of these "high" gravity stars is related to the systematic overestimation of $\log g$ by MD as discussed in Sect. 4.

We cannot confirm, in our range of gravity values, the discrepancy found by Balona (1994), the discrepancy being, at least partly, due to the use of old Kurucz models and the Lester et al. (1986) synthetic indices.

8.3. Mass-luminosity relation

In order to evaluate the possible dependency of mass values with respect to the adopted stellar models, we compared the masses, as computed in the previous section,

with those obtained by interpolating in the tracks by Bressan et al. (1993) and by Lebreton et al. (1997) using the CESAM code (Morel 1997). The differences between the masses computed from Schaller et al. (1992) and Bressan et al. (1993) have a mean value of -0.01 $\mathcal{M}/\mathcal{M}_{\odot}$ and for Lebreton computations, the differences have a mean value of 0.04 $\mathcal{M}/\mathcal{M}_{\odot}$, which is negligible for our analysis.

We underline the fact that through the Hipparcos experiment the $\mathcal{M}$-L relationship can be derived from non eclipsing field stars. This relation is illustrated in Fig. 11a. We note the very tight relationship between the two parameters, mass and luminosity, but we recall that they cannot be considered as being totally independent both relying upon M_V for their determination.

We have compared the relation derived from our sample of stars to the empirical one from binary systems (see Fig. 5 in Andersen 1991), also plotted in the same Fig. 11a. The general agreement appears clearly. Let us recall that our relation depends on stellar evolutionary models and that the relation based on eclipsing binaries is totally independent from a methodological point of view. Figure 11a shows that the gap around $\log \mathcal{M} = 0.5$ in the Andersen sample is filled by the present study.

Andersen (1991) pointed out a significant scattering of the points around the mean relation and related it to age and chemical composition effects on luminosity. The evolutionary effect on the stars of our sample is revealed by the $\log g$ parameter. If we split the stars of our and Andersen samples (in the $T_{\rm eff}$ range covered by A0 V stars) in narrow intervals of $\log\ g$ (see Fig. 11b), the dominant effect on the scatter is clearly related to gravity, since the mean relation for each group is smooth and better defined.

The use of the $\mathcal{M}$-L relationship to determine the mass of individual dwarf stars requires the knowledge of $\log g$, parameter decreasing with stellar age, even inside the stellar main sequence life as it can be seen Fig. 12 where the effect of evolution is emphasized by overplotting the values of mass and luminosity derived from evolutionary models. Only the points corresponding to the core hydrogen burning phase are displayed.

As a result the derived luminosity is directly related to the accuracy of the adopted $\log g$ value.

The masses extracted from an HR diagram $L-T_{\rm eff}$ coupled with evolutionary tracks does not need the knowledge of $\log\ g$ and allows to derive the mass of a star by taking into account its distance from the ZAMS. In this case the uncertainty on the mass depends on the reliability of the evolutionary tracks.

8.4. Ages

The ages of the non binary and non peculiar stars have been determined by interpolation through the evolutionary tracks in the HR diagram and are given in Col. 9 of Table 4, the errors are expressed in % in Col. 10.

There are 6 stars younger than 10^8 years.

From Table 4 and the corresponding Fig. 9 we note that a small number of objects are very near the ZAMS and may still preserve signs of their recent formation as, for instance, an IR excess. We underline once more that a significant number of slightly evolved stars is present among the A0 stars of luminosity class V.

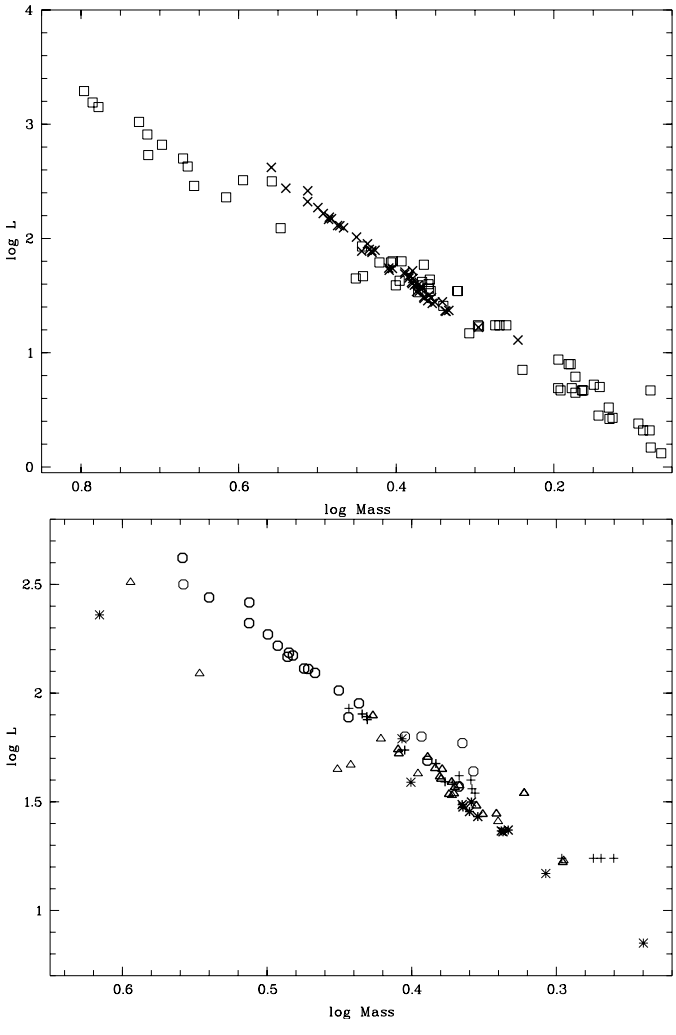

Fig. 11. a) The mass versus luminosity diagram for the stars of luminosity class V in our (×) and Andersen (square) samples. **b)** Zoom of the previous plot centered around A0 stars; the symbols are the same as in Fig. 9

8.5. Rotational velocities

We should not forget that a third parameter can affect the position of a star in the HR diagram: the rotational velocity. Such influence has been largely analysed from a theoretical point of view and recently studied, for stars hotter than those of the present paper, by Brown & Verschueren (1997).

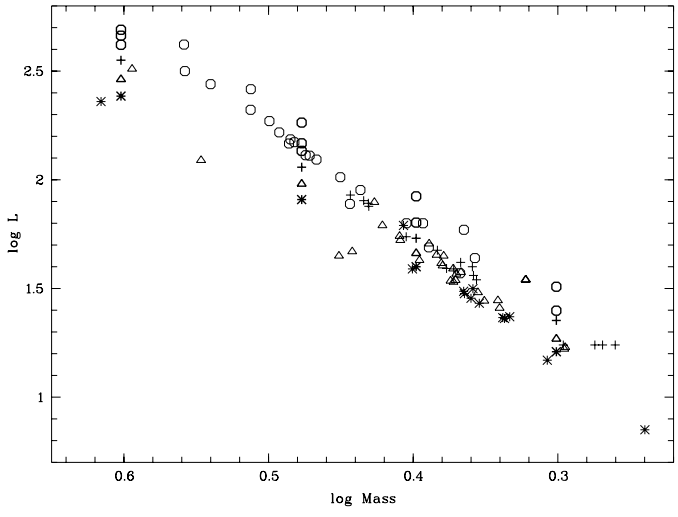

Fig. 12. The combined mass versus luminosity diagrams (same symbols as in Fig. 11b) on which the evolution of the luminosity for various masses (taken from Schaller et al. 1992, tables) is overplotted using the same symbols but with thick lines

We overplotted the observed spectra, after correction for RV, on the appropriate synthetic spectrum; the rotation value introduced in the computed spectrum that better fits the observations, is given in Col. 12 of Table 2, independent of the detection of established or suspected binarity. For some stars two values are given in the Table, when the v sin i was very uncertain; for HD 111786 the two values represent the velocities of the two components of the binary system. For the fastest rotators only H_γ and Mg II 4481 can be used for the comparison with computations.

We know that dwarf A-type stars are intrinsically fast rotators and generally characterized by mean-high values of v sin i, with an average value not lower than 100 $\mathrm{km\,s^{-1}}$. Stars with projected rotational velocities much lower than this value deserve some attention.

An account of the unknown parameter i, a low v sin i value may indicate that the object under study belongs to a class of the CP stars, is a close binary or is a Blue Horizontal Branch Star. From our sample we note that, among the 34 slowly rotating stars, 20 belong to one of the above categories.

The detection of binaries from broad lined spectra is more delicate and difficult; the availability of several orders of echelle spectra and the study of the cross correlation between observed and computed spectra has been fundamental for this detection.

Four of the observed stars belong to the Catalogue of v sin i standard stars by Slettebak et al. (1975). These stars are: HD 4150, HD 71155, HD 125473 and HD 188228.

9. Conclusion

Our aim was to define a set of "reference" dwarf A0 stars, having accurate parallaxes, in order to be combined with Vega in the role of "standard" stars.

The selection of non binary and non peculiar objects has been obtained from a selected sample of dwarf A0 extracted from Hipparcos Input Catalogue and observed spectroscopically. By combining photometric and spectroscopic informations with astrometric data and stellar evolutionary models, the original sample had to be reduced by 35%.

The inclusion of a Balmer line in the analysis of stellar spectra of A-type stars is not trivial, owing the small size of the CCD detectors, but the informations that can be extracted are often underestimated. In a binary system, the contamination detected on the combined spectrum, when the two components belong to similar spectral types and have a different radial velocity, is expected first on Balmer lines since these are the strongest features over a large temperature interval. The second key line is the Mg II doublet at 4481 Å; its intensity is barely dependent on temperature and gravity for stars from late B to early A stars. A broadening of this line different from that expected by rotation can be detected with the resolution $R = 28\,000$ in the spectra of stars with v sin i higher than 15 $\mathrm{km\,s^{-1}}$.

In the original sample of non evolved A-type stars, we have detected a fairly large number of new binary stars, as well as suspected ones (Sects. 5 and 6); we also have detected peculiar objects such as a shell star, hot Am stars and a misclassified object.

The masses and luminosities derived for the reduced sample of stars which can be considered as "normal" has allowed to fill up the gap of the classical $\mathcal{M}$-L relation obtained from eclipsing binaries and to point out the important role of accurate $\log g$ values to define this relation (Sect. 8). The agreement found between the evolutionary based surface gravity $\log g_{\mathrm{ev}}$ and the value of $\log g_{\mathrm{ph}}$ obtained from photometric data does not confirm the discrepancies found by Balona (1994) at least in our gravity range.

Independently of $\log g$, the masses can be derived directly from the $L - T_{\mathrm{eff}}$ HR diagram, but in this case the reliability of the evolutionary tracks becomes crucial.

In conclusion the two methods remain valid and complementary tools to determine the stellar masses.

Acknowledgements. The implementation of the Kurucz programs and the friendly help in using them by F. Castelli at Trieste has been highly appreciated. We would also thank P. Bonifacio for helpful suggestions and advices. We acknowledge A. Sellier for her technical assistance. Use was made of the SIMBAD data base, operated at the CDS, Strasbourg, France. Grants from MURST 40% and 60% are acknowledged.

Appendix

HD 3003 Short period binary; both components are of A-type, according to the BSC. An IR excess has been measured from IRAS data by Stencel & Backman (1992) and by Oudmaijer et al. (1992) who derived the [12]−[25] colour index = −1.15.

HD 4065 The spectra of the two components are A0 and A9, according to the BSC; the TD1 colours confirm that the secondary does not affect the UV colours. Recent speckle measures are given by Hartkopf et al. (1996) and by Horch et al. (1996).

HD 4150 The fit of the observed to the computed spectrum is such that this object is suspected to be a binary. Standard star for rotational velocity (Slettebak et al. 1975), but the $v \sin i = 105$ km s^{-1} value does not agree with that derived by (Levato 1972) $v \sin i = 60$ km s^{-1}.

HD 7916 The peculiar spectrum is discussed in the text. The B component is classified A8p? and its peculiarities ascribed to contamination by the brighter companion by Corbally (1984) who gives, for the V magnitudes of the components, $V_A = 6.42$ and $V_B = 8.26$.

HD 15004 Known shell star with a variable RV of the shell (Levato et al. 1995). Evidence of accreting, circumstellar gas from IUE spectra is discussed by Grady et al. (1996).

HD 21473 We note that among stars of our sample this is the "normal" star with the lowest $T_{\rm eff}$ value. The star has been tested for photometric variability with negative result by Jorgensen et al. (1971) and confirmed by Hipparcos photometric data.

HD 34968 Slight variability of spectral lines noted by Gray & Garrison (1987) on low resolution spectra. Photometric variable $V = 4.67 - 4.72$ (SIMBAD data base), while no photometric variability was detected by Jorgensen et al. (1971) and confirmed by Hipparcos photometric data. Old MK classifications give A0 V var.

The Mg II 4481 is slightly asymmetric on the two spectra at our disposal.

HD 38206 The abundance analysis has been made by Lemke (1989 and 1990); the abundances of N and S have been added by Rentzsch-Holm (1997).

HD 45557 (ESA 340) Large differences between the $T_{\rm eff}$ values derived from various indices have been found by Böhm-Vitense (1982), using visual and UV data. The other stars, in this paper, with similar $T_{\rm eff}$ discrepancies are close binaries or shell stars.

HD 63112 This star has a low $\log g$ value for its A0 V spectral classification. A search for binarity by speckle interferometry gave negative results.

HD 67725 The core of H_γ is too narrow for the 250 km s^{-1} (in agreement with the $v \sin i = 240$ km s^{-1} by Dworetsky 1974) fitted by the Mg II 4481 profile. The $\log g = 3.30$ derived from the MD procedure is the lowest of the sample and it is too low to fit the H_γ profile. Slight differences of Mg II 4481 profiles are detected on the two observed spectra.

HD 69589 An IRAS colour excess at 12 μm has been derived by Patten & Willson (1991).

HD 71043 Possible variability of the RV and large rotational velocity are noted by Andersen & Nordström (1983).

HD 71155 Standard star for $v \sin i$ (Slettebak et al. 1975). The IR excess detected from IRAS at 25 μm is interpreted as due to a dust shell (Coté 1987). In the UV, the m_{1565} is quite high compared with that of other stars of similar $T_{\rm eff}$ and to the computed colours; the UV flux below 2500 Å agrees with $T_{\rm eff} = 10000$ K, 250 K higher than that obtained from visual data. The four spectra taken by us show some peculiar line profiles.

HD 79108 An IR excess at 60 μm is derived from IRAS data (King 1994); the star is a λ Boo candidate, according to Maitzen & Pavlovski (1989).

HD 84461 We did not detect variations on the 3 spectra taken by us. The best fit with computations requires a lower $T_{\rm eff}$ (9500 K) than that derived from photometric colour indices.

HD 85504 The intriguing properties of this object are summarized by Cacciari (1985). An overabundance of He and C with respect to Sirius has been derived by Wallerstein et al. (1962) who formulate the hypothesis of a composite spectrum by a B8 and an A1 star.

Many metal lines are stronger in the observed, compared to the computed spectrum. We found many, but slight and difficult to prove, indications of binarity (e.g. the H_γ profile does not fit well those computed with the photometrically derived parameters; an abnormally large strength of many metal lines; the not rotationally broadened Mg II 4481 profile; the UV flux below 2500 Å fits that computed with $T_{\rm eff} = 10500$ K, while the $m_{2740} - V$ suggests $T_{\rm eff} = 10000$ K).

The spectral peculiarities are studied by Adelman & Pintado (1997).

HD 87344 The abundance analysis of this narrow-line star has been made by Lemke (1989 and 1990) and by

Rentzsch-Holm (1997). The other component of this visual system, HD 87330, has been recognized to be a SB2; it is identified as HD 87344(2) in the HM Catalog and its photometric values are not correct (see Text).

HD 92845 The TD1 colours are better fitted by undereddened colours.

HD 109573 Star of β Pic type with a very strong disk luminosity, even higher than that of β Pic itself; a recent discussion of this young object can be found in Mouillet et al. (1997). The spectrum is characterized by weak metal lines; in particular, the Mg II 4481 profile is weak and not rotationally broadened and the UV colours (Fig. 8a) do not fit those predicted with the atmospheric parameters given in Table 2. Moreover, the $\log g = 4.49$ derived from $uvby\beta$ photometry is too high for an A0 dwarf and does not fit the observed H_γ profile which better agrees with the $\log g = 4.30$ derived from the parameters obtained from the Geneva undereddened colour indices. The Napiwotzki et al. (1993) correction of the gravity determined by the MD programs gives $\log g = 4.43$, value that does not improve significantly the fit with the spectrum computed with the parameters derived from $uvby\beta$ colours.

HD 111519 The cross correlation has a low and flat central part; the Mg II 4481 has a composite profile with a sharp and a broad component, signature of a double-lined spectroscopic binary; the metal lines present an important veiling effect.

HD 111786 Binary λ Boo star discussed in the text and in Faraggiana et al. (1997). Among the stars of the present sample, this star has the lowest value of the cross correlation coefficient.

HD 114570 It has a very high colour excess, the H_γ profile is peculiar; it core suggests a $v \sin i$ lower than that obtained from metal lines and the UV dereddened colours fit better a $T_{\rm eff}$ lower by 250 K than that derived from visual data.

HD 125473 This star is classified A0 III by Gray & Garrison (1987). It is a dusty system on the basis of IRAS data (Cheng et al. 1992). We did not detect differences between the 5 spectra at our disposal. This is the star for which the highest difference in $T_{\rm eff}$ between MD and Geneva calibrations has been found; the H_γ profile is fitted by the spectrum computed with the MD parameters.

HD 129791 It is an X-ray source (Schmitt et al. 1993) difficult to explain since A0-type stars are not X-ray emitters. A relatively high dereddening is requested to reproduce the colours of a normal star. The lines are extremely broadened and their profile suggest a composite spectrum with different $v \sin i$ of the two components.

HD 139129 The abundance analysis has been made by Lemke (1989, 1990) who adopted $T_{\rm eff} = 9900$ K and $\log g = 3.7$ and derived non solar abundances for several elements. Further discussion on the metal abundances is in Rentzsch-Holm (1997). According to Jaschek et al. (1991), this star has an unexplained IR excess at 12 μm.

HD 151527 No meaningful M_V can be computed owing the high distorted colours from which large and discrepant colour excesses are derived (see Table 2). The peculiarity of the visual and UV colours and of the spectrum suggests that this object is more complex than a simple binary star. The UV TD1 colours are very distorted.

HD 152849 According to Richichi et al. (1997) discussion of this star, the companion has also a spectral type A and is only slightly later than the primary. Recent speckle measures are in Horch et al. (1996).

HD 188228 The $v \sin i$ value measured by Slettebak et al. (1975) ($v \sin i = 80$ km s^{-1}) does not agree with that obtained by Levato (1972) ($v \sin i = 140$ km s^{-1}). A variability is mentioned in old MK classifications.

The Mg II profile is not rotationally broadened; several metal lines have a flat core and the UV fits better $T_{\rm eff} = 10500$ K.

HD 193571 It is a protoplanetary system candidate on the basis of the IR excess detected by IRAS (Cheng et al. 1992); no signatures of CS features have been observed by Holweger & Rentzsch-Holm (1995).

HD 213320 It belongs to the hot extension of the Am sequence according to Adelman & Nasson (1980), but with several abundance anomalies (Adelman et al. 1984); it is an SB according to Dworetsky (1974).

HD 225200 Ambiguous classifications are found in the literature: it is a binary A0 V + A: according to Levato et al. (1979) and B9 IVs + A2n according to AM, but A0 IV$^-$(shell) according to Gray & Garrison (1987).

References

Abt H.A., Morrell N.I., 1995, ApJS 99, 135 [AM]
Adelman S.J., Nasson M.A., 1980, PASP 92, 346
Adelman S.J., Young J.M., Baldwin H.E., 1984, MNRAS 206, 649
Adelman S.J., Pintado O.I., 1997, A&AS 125, 219
Andersen J., 1991, A&AR 3, 91
Andersen J., Nordström B., 1983, A&AS 52, 471
Asiain, 1998, Ph Thesis Universitat de Barcelona
Balona L.A., 1994, MNRAS 268, 119
Bessell M.S., Castelli F., Plez B., 1998, A&A 333, 231 and 337, 321

Bressan A., Fagotto F., Bertelli G., Chiosi C., 1993, A&AS 100, 647
Böhm-Vitense E., 1982, ApJ 255, 191
Brown A.G.A., Verschueren W., 1997, A&A 319, 811
Burnage R., Gerbaldi M., 1990, 2nd ESO/ST-ECF Data Analysis Workshop, Baade D., Grøsbol P. (eds.). ESO Garching, p. 137
Burnage R., Gerbaldi M., 1992, 4nd ESO/ST-ECF Data Analysis Workshop, Grøsbol P., de Ruijsscher R.C.E. (eds.). ESO Garching, p. 159
Cacciari C., 1985, A&AS 61, 407
Castelli F., 1991, A&A 251, 106
Castelli F., Kurucz R.L., 1994, A&A 281, 817
Cayrel de Strobel G., 1996, A&AR 7, 243
Cheng K.P., Bruhweiler F.C., Kondo Y., Grady C.A., 1992, ApJS 396, L83
Collins G.W., II, Smith R.C., 1985, MNRAS 213, 519
Corbally C.J., 1984, ApJS 55, 657
Corbally C.J., 1987, ApJS 63, 365
Coté J., 1987, A&A 181, 77
Dworetsky M.M., 1974, ApJS 28, 101
Dworetsky M.M., Moon T.T, 1986, MNRAS 220, 787
ESA, The Hipparcos Catalogue, 1997, ESA SP-1200
Faraggiana R., Gerbaldi M., Burnage R., 1997, A&A 318, L21
Figueras F., Torra J., Jordi C., 1991, A&AS 87, 319
Gerbaldi M., Gómez A.E., Faraggiana R., et al., 1989, The Messenger 56, 12
Gerbaldi M., Faraggiana R., Burnage R., et al., 1998a, Contrib. Astron. Obs. Skalnaté Pleso 27, 197
Gerbaldi M., Faraggiana R., Burnage R., et al., 1998b, IAU Highlights (in press)
Grady C.A., Pérez M.R., Talavera A., et al., 1996, ApJ 471, L49
Gray R.O., Garrison R.F., 1987, ApJS 65, 581
Hartkopf W.I., Mason B.D., McAlister H.A., et al., 1996, AJ 111, 936
Hauck B., Mermilliod M., 1990, A&AS 86, 107 [HM]
Hoffleit D., Jaschek C., 1982, Bright Star Catalogue, Yale University Observatory [BSC]
Hoffleit D., Warren W.H., 1994, The Bright Star Catalogue, 5th revised ed., version 1994 June (private communication) [BSC1994]
Holweger H., Rentzsch-Holm I., 1995, A&A 303, 819
Horch E.P., Dinescu D.I., Girard T.M., et al., 1996, AJ 111, 1681
Jaschek C., Jaschek M., Andrillat Y., Egret D., 1991, A&A 252, 229
Jaschek C., Valbousquet A., 1997, A&AS 126, 251
Jordi C., Masana E., Figueras F., et al., 1997, A&AS 123, 83
Jorgensen H.E., Johansen K.T., Olsen E.H., 1971, A&A 12, 223
King J.R., 1994, MNRAS 269, 209
Künzli M., North P., Kurucz R.L., et al., 1997, A&AS 122, 51
Kurucz R.L., 1979, ApJS 40, 1
Kurucz R.L., 1993, CD Rom 13 and 18
Lebreton Y., Perrin M.-N., Fernandes J., et al., 1997, ESA SP-402, 379
Lemke M., 1989, A&A 225, 125
Lemke M., 1990, A&A 240, 331
Lester J.B., Gray R.O., Kurucz R.L., 1986, ApJS 61, 509
Levato O.H., 1972, PASP 84, 584
Levato O.H., Morrell N.I., Malaroda S., 1979, Rev. Mex. A. A. 4, 321
Levato O.H., Mallaroda S., Jaschek C., Jaschek M., 1995, A&A 299, 163
Maitzen H.M., Pavlovski K., 1989, A&AS 81, 335
Mermilliod J.-C., Mermilliod M., Hauck B., 1997, A&AS 124, 349
Moon T.T., 1985, Comm. from the Univ of London Obs. 78 and Revisions 1985 (private communication)
Moon T.T., Dworetsky M.M., 1985, MNRAS 217, 305 [MD]
Morel P.J., 1997, A&AS 124, 597
Mouillet D., Lagrange A.M., Beuzit J.L., Renaud N., 1997, A&A 324, 1083
Napiwotzki R., Schönberner D., Wenske V., 1993, A&A 268, 653
Oudmaijer R.D., van der Veen W.E.C.J., Waters L.B.F.M., et al., 1992, A&AS 96, 625
Patten B.M., Willson L.A., 1991, AJ 102, 323
Rentzsch-Holm I., 1997, A&A 317, 178
Richichi A., Calamai G., Leinert Ch., et al., 1997, A&A 322, 202
Schaller G., Schaerer D., Meynet G., et al., 1992, A&AS 96, 269
Schmitt J.H.M.M., Zinneker H., Cruddace R., Harnden F.R. Jr., 1993, ApJ 402, L13
Slettebak A., Collins II G.W., Boyce P.B., et al., 1975, ApJS l29, 137
Slettebak A., Kuzma T.J., Collins G.W. II, 1980, ApJ 242, 171
Smalley B., Dworetsky M.M., 1993, A&A 271, 515
Stencel R.E., Backman D.E., 1991, ApJS 75, 905
Strömgren B., 1966, ARA&A 4, 433
Turon C., Crézé M., Gómez A., et al., 1992, The Hipparcos Input Catalogue, ESA SP-1136
Thompson G.I., Nandy K., Jamar C., et al., 1978, Catalogue of Stellar Ultraviolet Fluxes The Science Research Council
Wallerstein G., Stone Y.H., Williams J.A., 1962, ApJ 135, 459